Applied Thermal Engineering 302 (2026) 131744

Contents lists available at ScienceDirect

Applied Thermal Engineering

journal homepage: www.elsevier.com/locate/apthermeng

Research Paper

Two-phase frictional pressure gradient correlation for saturated flow boiling in single circular and non-circular mini/ micro-channels

Sadaf Mehdi [a], Hyun Sung Hwang [a], V.S. Devahdhanush [b], Faraz Ahmad [a], Issam Mudawar [a,*], Arindom Joardar [c], Abdel Rahman Farraj [c], Mihajlo Golubovic [c], Asad M. Sardar [c]

[a] Purdue University Boiling and Two-Phase Flow Laboratory (PU-BTPFL), School of Mechanical Engineering, Purdue University, 585 Purdue Mall, West Lafayette, IN 47907, USA

[b] Department of Mechanical & Materials Engineering, University of Nebraska-Lincoln, Lincoln, NE 68588, USA

[c] Carrier Corporation, Indianapolis, IN 46231, USA

ARTICLE INFO

Keywords:
Saturated flow boiling
Pressure drop
Predictive correlation
Low-GWP refrigerants

ABSTRACT

Accurate prediction of two-phase frictional pressure gradients is crucial for operating two-phase flow systems within safe limits. However, existing correlations predict with high mean absolute errors (MAEs) especially for new low-GWP refrigerants, for instance, 53% for R1234yf and 41% for R32. To overcome this challenge, the present study developed a new correlation for frictional pressure gradient for mini/micro-channels applicable to both conventional and low-GWP working fluids. The correlation incorporates the effects of channel geometry, heat flux, inertial forces, and viscous forces through several dimensionless parameters including aspect ratio, heated-to-wetted perimeter ratio, boiling number, liquid-only Weber number, liquid-only Reynolds number, liquid-to-vapor density ratio, and two-phase Prandtl number. The amassed database consists of 3473 data points, of which 2882 are for circular and 591 are for non-circular cross-sectional geometries. The database encompasses flow boiling of 17 different fluids in single circular and non-circular mini/micro-channels of 0.529–8 mm hydraulic diameters with a mass velocity range of 33–2738 kg/(m^2.s). This database is used to evaluate the predictive performance of 18 existing correlations. Following this assessment, a new universal correlation is developed using nonlinear optimization on the consolidated database. The new correlation accurately predicts both circular and non-circular channels with respective MAEs of 19.22% and 23.13%, and using the entire combined database yields an MAE of 19.88%.

1. Introduction

In recent years, high power devices have become ubiquitous and are undergoing further rapid advancement and miniaturization. Thermal management of these devices poses a significant challenge as conventional single-phase cooling is no longer sufficient to handle such high heat fluxes [1]. Similarly, HVAC industry is also unable to meet the rising demand of compact and efficient heat exchangers using conventional single-phase techniques. These limitations have made two-phase cooling the prime candidate for such applications, due to its ability to exploit the coolant's latent heat of vaporization. Two-phase cooling can be achieved using various techniques such as flow boiling [2], pool boiling [3], spray [4,5] and jet impingement cooling [6]. Among these, flow boiling in mini/micro-channels offers a large heat dissipation potential in a very small space with much less coolant as compared to single-phase convection [7]. However, pressure losses are significantly higher in mini/micro-channels due to their small geometries [8]. Frictional pressure loss is usually the largest component due to the interaction between the two phases. Thus, accurate prediction of frictional pressure drop is essential for successful implementation of two-phase cooling in above applications.

1.1. Predicting frictional pressure gradients

To predict the frictional pressure gradient, various researchers have developed empirical/semi-empirical correlations. In 1949, Lockhart and Martinelli [9] proposed one of the first correlations for adiabatic flows. Later in 1979, Friedel [10] proposed an improved correlation for air-water flows in vertical and horizontal orientations. Using Lockhart and Martinelli's parameters, in 1986, Muller and Heck [11] proposed a new functional form to predict frictional pressure drops for air-water

* Corresponding author.
E-mail address: mudawar@ecn.purdue.edu (I. Mudawar).

https://doi.org/10.1016/j.applthermaleng.2026.131744
Received 12 February 2026; Received in revised form 15 May 2026; Accepted 1 June 2026
Available online 9 June 2026

Nomenclature

A_c	cross-sectional area of channel [m^2]
Bd	Bond number, $g(\rho_f - \rho_g)D_h^2/\sigma$
Bo	boiling number, q''_w/Gh_{fg}
C	empirical constant
c_p	specific heat at constant pressure [J/(kg.K)]
D	diameter [m]
D_h	hydraulic diameter, $4A_c/P_h$ [m]
f	Fanning friction factor
G	mass velocity [kg/(m^2.s)]
g	gravitational acceleration [m/s^2]
H	height of the non-circular channel's cross section [m]
h	enthalpy [J/kg]
h_{fg}	latent heat of vaporization [J/kg]
j	superficial velocity [m/s]
L	length [m]
MAE	mean absolute error [%]
$\dot{m}$	mass flow rate [kg/s]
N	number of data points
N_{conf}	confinement number, $\{\sigma/g(\rho_f - \rho_g)D_h^2\}^{1/2} = Bd^{-1/2}$
P_f	frictional perimeter of channel [m]
P_h	heated perimeter of channel [m]
Pr_{tp}	Two-phase Prandtl number, $x.Pr_g + (1\text{-}x)Pr_f$
p	pressure [Pa]
p_{crit}	critical pressure of fluid [Pa]
p_r	reduced pressure, p/p_{crit}
Δp	pressure drop [Pa]
q''	heat flux [W/m^2]
Re	Reynolds number
Su_{go}	vapor-only Suratman number, $\rho_g \sigma D_h/\mu_g^2$
T	temperature [°C]
v	specific volume [m^3/kg]
v_{fg}	specific volume difference between liquid and vapor [m^3/kg]
W	width of the non-circular channel's cross section [m]
We_{fo}	liquid-only Weber number, $G^2D_h/\sigma\rho_f$
X	Lockhart-Martinelli parameter
x	thermodynamic equilibrium quality, $(h - h_f)/h_{fg}$
z	streamwise coordinate [m]

Greek symbols

α	void fraction
β	channel aspect ratio, W/H
λ	dimensionless group in Lee and Lee correlation
μ	dynamic viscosity [kg/m.s]
μ_{tp}	two-phase mixture viscosity [kg/m.s]
ξ_{30}	percentage of data predicted within ±30% of experimental value
ρ	density [kg/m^3]
σ	surface tension [N/m]
φ	two-phase pressure drop multiplier
ψ	dimensionless group in Lee and Lee correlation
ω	parameter in Beattie and Whalley two-phase mixture viscosity model

Subscripts

A	accelerational component
e	equivalent
exp	experimental
F	frictional component
f	saturated liquid; single-phase liquid; bulk fluid
G	gravitational component
g	saturated vapor
go	vapor only
h	heated
in	inlet to channel's heated section
k	index for a phase: liquid (f) or vapor (g)
out	outlet of channel's heated section
$pred$	predicted
sat	saturation
sb	saturated boiling
sp	single-phase
tot	total
tp	two-phase
tt	turbulent-liquid, turbulent vapor
tv	turbulent-liquid, laminar vapor
vt	laminar-liquid, turbulent vapor
vv	laminar-liquid, laminar-vapor
w	channel wall

Acronyms

ANN	Artificial Neural Network
BNN	Bayesian Neural Network
GWP	Global Warming Potential
HVAC	Heating Ventilation and Airconditioning
HEM	Homogeneous Equilibrium Model
MCHX	Microchannel heat exchanger
MCMC	Markov Chain Monte Carlo
PAML	Physics-assisted Machine Learning
PU-BTPFL	Purdue University Boiling and Two-Phase Flow Laboratory
SFM	Separated Flow Model

and halocarbon flows in tubes of 4–392 mm diameter. Various other models and correlations were developed; those until 2013 are summarized in Kim and Mudawar's review article [7].

Later in 2016, Keepaiboon et al. [12] investigated the flow boiling of R134a in a single rectangular microchannel with a hydraulic diameter of 0.68 mm. Experiments were conducted over a mass flux range of 600–1400 kg/(m^2.s) and a heat flux range of 7.6–49 kW/m^2. Following the separated flow model (SFM) approach, they proposed a correlation for the parameter C based on Re_{fo}, Co, and X, which predicted the experimental data with a mean absolute error (MAE) of 4.7%. In the same year, Rollmann and Spindler [13] proposed a homogeneous equilibrium model (HEM)-based correlation for flow boiling in a microfin tube with a hydraulic diameter of 8.95 mm. Their experiments, conducted using R407C and R410A, covered a mass flux range of 62.5–1400 kg/(m^2.s) and resulted in a database of 952 data points. The proposed correlation predicted the data with an MAE of 18.1%. In 2018, Pan et al. [14] developed an HEM correlation based on an experimental dataset of approximately 100 data points. They investigated the flow boiling of deionized water in a microchannel with a hydraulic diameter of 0.1875 mm. A correlation for the two-phase multiplier was proposed by relating it to vapor quality, Weber number, liquid-to-vapor density ratio, vapor-to-liquid dynamic viscosity ratio, and the ratio of single-phase friction factors for vapor-only and liquid-only flows. The proposed correlation predicted their experimental dataset with an MAE of 12.23%. In 2021, Zeng et al. [15] developed a correlation to predict both boiling and adiabatic flow pressure drop of R32 in microchannels with hydraulic diameters ranging from 0.643 to 6 mm. The correlation was formulated using 496 data points compiled from eight independent studies and achieved an MAE of 17.86%. More recently, in 2023, Nie et al. [16] developed a correlation applicable to condensing, adiabatic, and boiling flows. Similarly, Moradkhani et al. [17] proposed a correlation for condensing and boiling flows. Both studies employed genetic programming techniques to derive their respective correlations.

While these correlations offer good predictions on the respective reported dataset, they are incapable of predicting the present flow boiling database. This potentially hinders their applicability to boiling-specific analysis due to differences in flow regimes between boiling and condensing/adiabatic flows [8]. As depicted in the flow schematics and experimentally obtained high-speed flow images in Fig. 1 [18,19], flow boiling features entrained liquid droplets in the central vapor core, which is absent in both condensing and adiabatic flows. It is imperative to seek a separate correlation to accurately predict the frictional pressure gradient for saturated flow boiling in mini/micro-channels. Based on this philosophy, in 2013, Kim and Mudawar [8] developed a universal correlation for frictional pressure drop for saturated flow boiling in mini/micro-channels.

1.2. Machine learning-based predictive models

Recent advances in machine learning have led to its increasing applications in the area of thermal sciences [21]. Neural networks based models have been extensively employed in the prediction of CHF [22], Pressure drop [2], and heat transfer coefficient [23]. In the area of pressure drop predictions, Qiu et al. [24] developed several machine learning based models including artificial neural network (ANN), K-nearest neighbors, XGBoost, and LightGBM using the consolidated database of 2787 data points and obtained an MAE of 9.58% using ANN on the test data set. Similarly, Mudawar et al. [25] developed an ANN-based predictive framework to estimate pressure drop during flow boiling under microgravity conditions aboard the International Space Station. Their model showed excellent predictive capability, with an MAE of 5.24% on the test dataset. ANN models have demonstrated strong predictive capability when sufficient high-quality data are available.

However, several limitations arise when employing purely data-driven machine learning approaches. First, conventional neural networks typically provide only point estimates and do not quantify the uncertainty associated with their predictions. This lack of uncertainty information can be a significant limitation, particularly in the design of critical thermal systems, where confidence in the prediction is as important as the predicted value itself. To address this limitation, many researchers have proposed incorporating a Bayesian framework into neural networks, leading to the development of Bayesian Neural Networks (BNNs) [26].

In this approach, model parameters are treated as probability distributions rather than deterministic values, enabling direct quantification of predictive uncertainty. However, exact Bayesian inference in neural networks is generally intractable due to the high dimensionality of the parameter space. Consequently, approximate inference techniques are employed, most commonly Markov chain Monte Carlo (MCMC) [26] and stochastic gradient MCMC [27] which allow practical estimation of posterior distributions. These methods enable neural networks to address uncertainty-related limitations by providing both predictive estimates and associated confidence intervals.

These methods enable the model to address the uncertainty concerns associated with neural network predictions by providing both prediction and confidence interval. In this context, Colak et al. [28] developed a Bayesian-regularized artificial neural network model to predict pressure drop during the condensation and evaporation of R134a in a vertically oriented smooth copper tube. The proposed model demonstrated strong predictive performance, achieving MAEs of 7.5% and 8.9% on the test datasets for condensation and evaporation, respectively.

Beyond uncertainty quantification, another key limitation of purely data-driven models is their lack of physical interpretability, as their predictions are often governed primarily by statistical fitting rather than underlying transport mechanisms. To address this challenge, so-called *physics-assisted* machine learning (PAML) models have recently emerged and are gaining increasing attention within the two-phase flow community [29,30]. Given the highly complex and nonlinear nature of two-phase flow, it remains difficult to directly embed the full governing physics into a machine learning framework. Consequently, PAML approaches typically incorporate physics through established empirical or semi-empirical correlations. In these frameworks, a selected correlation provides an initial baseline prediction, while the machine learning

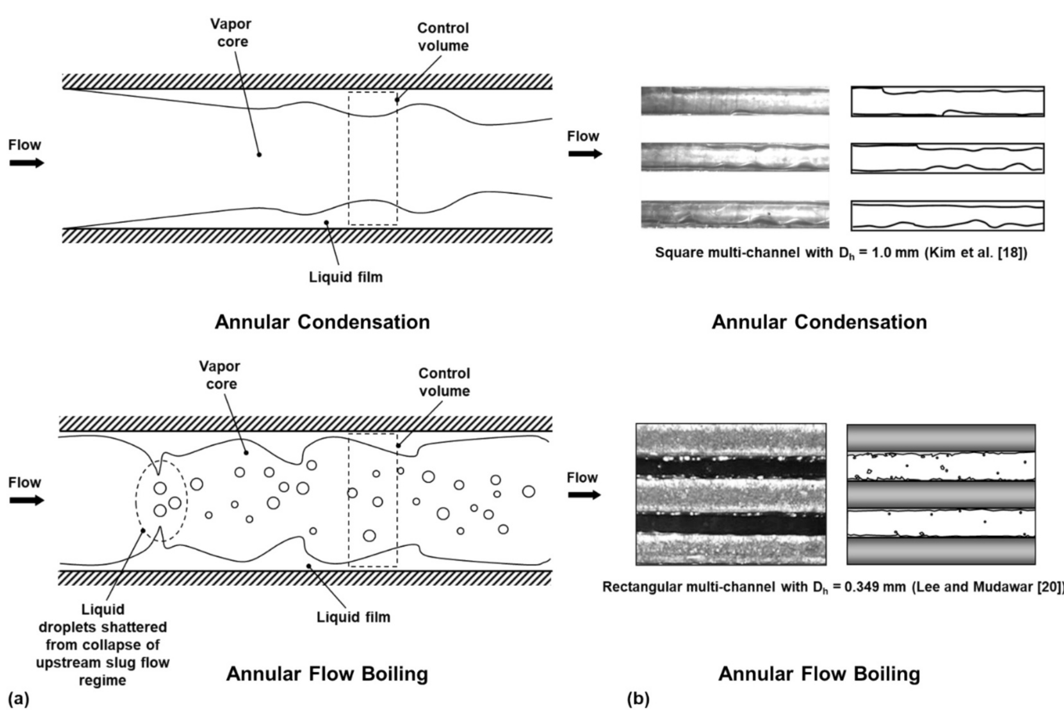

Fig. 1. (a) Fundamental flow structural difference in annular flow condensation [18] and annular flow boiling [20]. (b) Actual experimental photographs (left) and schematics (right). Adapted from Kim and Mudawar [8].

model is trained to learn the residuals between the correlation-based estimates and experimental data, thereby improving the overall predictive accuracy.

For example, Golezani et al. [31] developed a PAML framework to predict condensation pressure drop in mini/microchannels by training an XGBoost model on the residuals of the separated flow model (SFM)-based correlation proposed by Kim and Mudawar [32]. The proposed model achieved a MAE in the range of 7.4–8.3%. Their results demonstrated that physics-assisted frameworks can provide more accurate and physically informed predictions compared to purely data-driven machine learning models.

These developments underscore that the formulation of robust empirical and semi-empirical correlations remains fundamentally important, not only for direct engineering applications, but also as a physically grounded foundation for hybrid and machine learning-based predictive frameworks.

1.3. Objectives of study

The present study builds on the classical Kim and Mudawar's [8] framework in which flow boiling is treated separately from condensing/adiabatic flows because of the fundamental differences in two-phase flow structure. The objective of this study is to consolidate the global database for flow boiling in single mini/micro-channels including new low-GWP refrigerants and develop a more accurate universal predictive correlation for frictional pressure gradient. The database consists of 2882 data points collected from 19 studies on 13 different fluids in single circular mini/micro-channels, along with 591 data points from 5 studies on 8 fluids in non-circular mini/micro-channels. Existing homogeneous equilibrium model (HEM)-based and separated flow model (SFM)-based correlations are assessed against the consolidated database, and a new universal correlation capable of accurately predicting both geometries is developed by employing the same methodology as prior PU-BTPFL studies on predicting pressure drop [7,33].

It should be emphasized that the present work does not aim to develop a machine learning based predictive model. The discussion of machine learning based models in the literature is included only to provide context on most recent data driven approaches for two-phase frictional pressure gradient prediction. The scope of this study is limited to the assessment and development of a physically guided seminal empirical universal correlation for prediction of saturated flow boiling frictional pressure gradient.

1.4. Key contribution

The present study develops a generalized correlation for saturated flow boiling frictional pressure gradient using a substantially extended database of 3473 data points as compared to the 2033 data points of Kim and Mudawar's [8] study on single mini/microchannels. The Chisholm parameter C is reformulated through the inclusion of channel aspect ratio and quality-weighted two-phase Prandtl number. The aspect ratio accounts for geometric effects in non-circular channels, whereas Pr_{tp} represents the combined influence of thermophysical properties of fluids during boiling flows. These parameters are not explicitly included in the original Kim and Mudawar's [8] correlation and are introduced here to improve predictability across broad geometries and refrigerant property ranges. The coefficients and exponents of the proposed formulation are optimized using the full consolidated database by minimizing the MAE between the predicted and experimental frictional pressure gradient. Consequently, the applicability of proposed correlation is extended to modern low-GWP refrigerants and non-circular mini/micro-channels.

2. Existing predictive methods for two-phase pressure drop

The total two-phase pressure drop is the sum of frictional, gravitational and accelerational components,

$$\Delta p_{tp} = \Delta p_{tp,F} + \Delta p_{tp,A} + \Delta p_{tp,G} \tag{1}$$

2.1. Frictional pressure gradient

Frictional pressure gradient is calculated using the Homogeneous Equilibrium Model (HEM) or the Separated Flow Model (SFM).

HEM provides a relation:

$$-\left(\frac{dp}{dz}\right)_F = \frac{2 f_{tp} v_f G^2}{D_h}\left(1 + x\frac{v_{fg}}{v_f}\right) \tag{2}$$

where two-phase friction factor, f_{tp}, is calculated for circular channels as:

$$f_{tp} = \begin{cases} 16 Re_{tp}^{-1}, & Re_{tp} < 2000 \\ 0.079 Re_{tp}^{-0.25}, & 2000 \le Re_{tp} < 20000 \\ 0.046 Re_{tp}^{-0.2}, & Re_{tp} \ge 20000 \end{cases} \tag{3}$$

and for rectangular channels of width W, height H, and aspect ratio $\beta = W/H$:

$$f_{tp} = \begin{cases} 24\begin{pmatrix} 1 - 1.3553\beta + 1.9467\beta^2 - 1.7012\beta^3 \\ +0.9564\beta^4 - 0.2537\beta^5 \end{pmatrix} Re_{tp}^{-1}, & Re_{tp} < 2000 \\ 0.079 Re_{tp}^{-0.25}, & 2000 \le Re_{tp} < 20000 \\ 0.046 Re_{tp}^{-0.2}, & Re_{tp} \ge 20000 \end{cases}. \tag{4}$$

Two-phase Reynolds number, Re_{tp}, is defined as:

$$Re_{tp} = \frac{G D_h}{\mu_{tp}} \tag{5}$$

where two-phase mixture viscosity, μ_{tp}, is obtained via relations reported in the literature [34–41].

Some widely used relations are listed in Table 1.

The SFM-based approach is also widely used to calculate frictional pressure gradient. The main difference between HEM and SFM is that SFM treats the two phases separately and thus individual phase equations are solved to estimate the pressure drop. Lockhart-Martinelli [9] proposed one of the first SFM-based models, where frictional pressure gradient is obtained by multiplying the single-phase pressure gradient with a two-phase multiplier, φ_k, as:

$$-\left(\frac{dp}{dz}\right)_F = \begin{cases} -\left(\frac{dp}{dz}\right)_{F,f}\varphi_f^2, & -\left(\frac{dp}{dz}\right)_{F,f}\varphi_f^2 > -\left(\frac{dp}{dz}\right)_{F,g}\varphi_g^2 \\ -\left(\frac{dp}{dz}\right)_{F,g}\varphi_g^2, & -\left(\frac{dp}{dz}\right)_{F,g}\varphi_g^2 > -\left(\frac{dp}{dz}\right)_{F,f}\varphi_f^2 \end{cases} \tag{6}$$

The individual phase frictional pressure gradients for liquid (f) and

Table 1
Summary of HEM-based two-phase mixture viscosity models.

Author(s) (Year)	Equation(s)
McAdams et al. (1942) [34]	$\frac{1}{\mu_{tp}} = \frac{x}{\mu_g} + \frac{1-x}{\mu_f}$
Davidson et al. (1943) [35]	$\mu_{tp} = \mu_f\left[1 + x\frac{v_{fg}}{v_f}\right]$
Akers et al. (1959) [36]	$\mu_{tp} = \frac{\mu_f}{(1-x) + x\left(v_g/v_f\right)^{0.5}}$
Cicchitti et al. (1960) [37]	$\mu_{tp} = x\mu_g + (1-x)\mu_f$
Owens (1961) [38]	$\mu_{tp} = \mu_f$
Dukler et al. (1964) [39]	$\mu_{tp} = \frac{xv_g\mu_g + (1-x)v_f\mu_f}{xv_g + (1-x)v_f}$
Beattie & Whalley (1982) [40]	$\mu_{tp} = \omega\mu_g + (1-\omega)(1+2.5\omega)\mu_f$ $\omega = \frac{xv_g}{v_f + xv_{fg}}$
Lin et al. (1991) [41]	$\mu_{tp} = \frac{\mu_f\mu_g}{\mu_g + x^{1.4}\left(\mu_f - \mu_g\right)}$
Awad and Muzychka (2008) [42]	$\mu_{tp} = \mu_g\frac{2\mu_g + \mu_f - 2\left(\mu_g - \mu_f\right)(1-x)}{2\mu_g + \mu_f + \left(\mu_g - \mu_f\right)(1-x)}$

vapor (g) are calculated as:

$$-\left(\frac{dp}{dz}\right)_{F,f} = \frac{2f_f G^2(1-x)^2 v_f}{D_h} \tag{7}$$

$$-\left(\frac{dp}{dz}\right)_{F,g} = \frac{2f_g G^2 x^2 v_g}{D_h} \tag{8}$$

where the friction factor for a phase k ($= f$ for liquid and g for vapor) is given by:

$$f_k = \begin{cases} 24\begin{pmatrix} 1 - 1.3553\beta + 1.9467\beta^2 - 1.7012\beta^3 \\ +0.9564\beta^4 - 0.2537\beta^5 \end{pmatrix} Re_k^{-1}, & Re_k < 2000 \\ 0.079Re_k^{-0.25}, & 2000 \le Re_k < 20000 \\ 0.046Re_k^{-0.2}, & Re_k \ge 20000 \end{cases} \tag{9}$$

Reynolds numbers for each phase are calculated as:

$$Re_f = \frac{(1-x)GD_h}{\mu_f} \tag{10}$$

$$Re_g = \frac{xGD_h}{\mu_g} \tag{11}$$

The two-phase multiplier is obtained as

$$\varphi_f^2 = 1 + \frac{C}{X} + \frac{1}{X^2} \text{ for liquid and} \tag{12}$$

$$\varphi_g^2 = 1 + CX + X^2 \text{ for vapor} \tag{13}$$

where Lockhart-Martinelli parameter, X, is given as

$$X = \left[-\left(\frac{dp}{dz}\right)_{F,f} \Big/ -\left(\frac{dp}{dz}\right)_{F,g}\right]^{0.5} \tag{14}$$

C is an empirical constant which is tuned according to the available experimental data. Numerous empirical correlations to estimate C are available in the literature. A list of commonly used correlations employing the SFM approach are listed in Table 2 and Table 3.

2.2. Accelerational and gravitational pressure gradients

Accelerational pressure gradient is calculated as:

$$-\left(\frac{dp}{dz}\right)_A = G^2\frac{d}{dz}\left[\frac{x^2}{\alpha\rho_g} + \frac{(1-x)^2}{(1-\alpha)\rho_f}\right], \tag{15}$$

where void fraction, α, is calculated using Zivi's correlation [43] for SFM as below:

$$\alpha = \left[1 + \left(\frac{1-x}{x}\right)\left(\frac{\rho_g}{\rho_f}\right)^{2/3}\right]^{-1} \tag{16}$$

and is derived from HEM as:

$$\alpha = \left[1 + \left(\frac{1-x}{x}\right)\left(\frac{\rho_g}{\rho_f}\right)\right]^{-1} \tag{17}$$

Gravitational pressure gradient is expressed as:

$$-\left(\frac{dp}{dz}\right)_G = g\sin\theta\left[\alpha\rho_g + (1-\alpha)\rho_f\right] \tag{18}$$

where θ is the channel inclination angle.

For the assessment of separated flow model (SFM) correlations, the parameter C is first evaluated using the correlations listed in Tables 2 and 3. Depending on the selected correlation, the predicted value of C is then incorporated into Eqs. (12) or (13) to determine the two-phase multiplier. The single-phase frictional pressure gradient is calculated using Eqs. (7)–(11). Subsequently, the two-phase frictional pressure gradient is obtained by multiplying the single-phase frictional pressure gradient with the predicted two-phase multiplier, as given in Eq. (6). The accelerational pressure gradient component is evaluated using Eq. (15). The void fraction required in this calculation is determined using Zivi void fraction correlation [43], which has been shown to provide reasonable agreement compared to other slip-based void fraction models [8]. Finally, the accelerational component is subtracted from the total pressure gradient to isolate the frictional pressure gradient.

It is necessary to subtract these losses before evaluating the frictional pressure gradient correlations because contribution of these losses varies. For instance, in Kharangate et al. (2012) [44] study on the one-sided heated upflow boiling of FC-72 in a 2.5 × 5 mm rectangular channel, the accelerational pressure gradient accounts for 17 to 36% of the total pressure gradient. The gravitational pressure gradient contribution ranges from 4.77% to 62.72% with an average of 16.96%. On the other hand, in the Keepaiboon et al. (2016) [12] study on the boiling flow of R134a in micro-channel under horizontal orientation, the accelerational pressure gradient contribution varied between ~1 to 12% because of the shorter heated length and different operating conditions.

2.3. Mechanistic models

In addition to HEM and SFM approaches, flow pattern-based models have also been developed for predicting two-phase pressure drop. Unlike purely empirical correlations, these models are derived from phase-wise momentum balances and require closure relations for interfacial shear stress, wall shear stress, void fraction, liquid film thickness, as well as droplet entrainment and deposition. One of the earlier models of this type was developed by Moreno and Thome [58] for horizontal evaporating flows. Their approach correlated pressure drop with the local interfacial structure, which was identified using the flow-pattern map proposed by Wojtan et al. [59]. The model was developed using a database of 1745 data points for the evaporation of R134a, R22, and R410A in tubes with diameters ranging from 8 to 13.8 mm. Their model successfully predicted 82.3% of the database within an error band of ±30%.

Subsequently, Cheng et al. [60] extended the Moreno and Thome framework to Carbon dioxide evaporating flow in tubes with diameters ranging from 0.8 to 7 mm. Their database comprised 387 data points collected from five independent studies, covering a mass flux range of 190–400 kg/(m^2.s). The proposed model predicted annular, dryout, and mist flow regimes with accuracies of 75.7%, 74.6%, and 75%, respectively. Following Thome's framework, Shiferaw et al. [61] proposed a semi-mechanistic model to estimate pressure drop during the boiling of R134a in tubes with diameters ranging from 0.52 to 4.26 mm. The model is applicable to the confined bubbly and slug flow regimes, covering vapor qualities up to 0.6 and mass fluxes between 100 and 500 kg/(m^2.s). The model predicted the experimental data with MAEs of 23%, 20%, 16.8%, 16.3%, and 22% for tube diameters of 4.26, 2.88, 2.01, 1.1, and 0.52 mm, respectively. The authors noted that the model loses validity as the flow transitions towards annular or dryout regimes.

Lee and Mudawar [62] developed a control-volume-based annular flow model for saturated flow boiling of R134a in a 609.6 mm long and 203.2 mm wide microchannel heat sink comprising 100 parallel channels of 1 × 1 mm^2 cross-section. Their model accounts for liquid film behavior, droplet entrainment and deposition, as well as turbulence effects in the vapor core through eddy momentum diffusivity. The proposed model predicted the experimental data with an MAE of 16.22%, with 97.10% and 100% of the data falling within error bands of ±30% and ± 50%, respectively.

Mauro et al. [63] proposed a mechanistic model for adiabatic symmetric annular flow with droplets entrainment. They amassed the database of 2992 data points from 11 studies spanning 7 fluids, while the final model assessment was performed using the annular flow subset selected based on void fraction greater than 0.70 criterion. Adopting approach similar to Wallis [64], they derived a relation for the friction factor by introducing a correction factor as a multiplier with the Blasius correlation [65], thereby accounting the effect of wavy interface. The correction factor was fitted using liquid-film Reynolds number. The proposed model predicted the pressure gradient with MAE of 19.4% and independent database with MAE of 19.3%. Expanding on their previous work, most recently, Mauro et al. [66] proposed an improved mechanistic pressure drop gradient and void fraction model for adiabatic annular flow. They amassed a consolidated annular flow database of 6377 data points from 37 studies spanning 23 fluids with $x > 0.25$. The

Table 2
Summary of SFM-based empirical correlations developed for adiabatic flow.

Author(s) (Year)	Equation(s)	Database of Development
Lockhart & Martinelli (1949) [9]	$C = \begin{cases} 20, & Re_f \geq 2000, Re_g \geq 2000 (tt) \\ 10, & Re_f \geq 2000, Re_g < 2000 (tv) \\ 12, & Re_f < 2000, Re_g \geq 2000 (vt) \\ 5, & Re_f < 2000, Re_g < 2000 (vv) \end{cases}$	• Adiabatic flow • Fluids: water, oil, kerosene, benzene • Shape: circular • Diameter: 1.49–25.83 mm
Mishima & Hibiki (1996) [45]	$C = \begin{cases} 21(1 - \exp(-0.319 D_h)), & \text{rectangular channel} \\ 21(1 - \exp(-0.333 D)), & \text{circular channel} \end{cases}$ Note that in this correlation, units of D_h and D are in mm.	• Adiabatic flow • Fluids: ammonia-vapor, air-water, ammonia-vapor, R113-N_2 • Shape: circular • Diameter: 0.7–25.37 mm
Lee & Lee (2001) [46]	$C = \begin{cases} 0.048 Re_{fo}^{0.451}, & Re_f \geq 2000, Re_g \geq 2000 (tt) \\ 3.627 Re_{fo}^{0.174}, & Re_f \geq 2000, Re_g < 2000 (tv) \\ 6.185 \times 10^{-2} Re_{fo}^{0.726}, & Re_f < 2000, Re_g \geq 2000 (vt) \\ 6.833 \times 10^{-8} \lambda^{-1.317} \psi^{0.719} Re_{fo}^{0.557}, & Re_f < 2000, Re_g < 2000 (vv) \end{cases}$	• Adiabatic flow • Fluid: air-water • Shape: non-circular • Hydraulic diameter: 0.78–6.67 mm
Yang & Webb (1996) [47]	$\left(\frac{dp}{dz}\right)_F = -0.87 Re_e^{0.12} f_{fo} \frac{G_{eq}^2 v_f}{D_h}; Re_{eq} = \frac{G_{eq} D_h}{\mu_f}; G_{eq} =$ $G\left[(1-x) + x\left(\frac{\rho_f}{\rho_g}\right)^{0.5}\right]$	• Adiabatic flow • Fluid: R12 • Shape: circular and non-circular • Hydraulic diameter: 1.56 and 2.64 mm
Wang et al. (1997) [48]	For $G \geq 200$ kg/(m^2.s), $\left(\frac{dp}{dz}\right)_F = \left(\frac{dp}{dz}\right)_g \varphi_g^2; \varphi_g^2 = 1 + 9.4X^{0.62} + 0.564X^{2.45}$ For $G < 200$ kg/(m^2.s), $\left(\frac{dp}{dz}\right)_F = \left(\frac{dp}{dz}\right)_f \varphi_f^2; \varphi_f^2 = 1 + \frac{C}{X} + \frac{1}{X^2};$ $C = 4.566 \times 10^{-6} X^{0.128} Re_{fo}^{0.938} \left(\frac{v_f}{v_g}\right)^{2.15} \left(\frac{\mu_f}{\mu_g}\right)^{5.1}$	• Adiabatic flow • Fluid: R22, R134a, R407C • Shape: circular • Diameter: 6.5 mm
Li & Wu (2010) [49]	$\left(\frac{dp}{dz}\right)_F = \left(\frac{dp}{dz}\right)_f \varphi_f^2; \varphi_f^2 = 1 + \frac{C}{X} + \frac{1}{X^2};$ For $Bd \leq 1.5$, $C = 11.9 Bd^{0.45}$ For $1.5 < Bd \leq 11$, $C = 109.4 \left(Bd Re_f^{0.5}\right)^{-0.56}$ For Bd>1, use HEM with Beattie & Whalley's [40] μ_{tp} relation	• Adiabatic flow • Fluids: R134a, R245fa, R236ea, R410a, R22, R404a, R12, R422d, R32, ammonia, propane, N_2. • Shape: circular and non-circular • Hydraulic diameter: 0.148–3.25 mm
Li & Wu (2011) [50]	For Bs<0.1, $\left(\frac{dp}{dz}\right)_F = \left(\frac{dp}{dz}\right)_f \varphi_f^2; \varphi_f^2 = 1 + \frac{C}{X} + \frac{1}{X^2}; C = 5.60 Bd^{0.28}$ For $Bd \geq 0.1$ and $Bd Re_f^{0.5} \leq 200$, $\left(\frac{dp}{dz}\right)_F = \left(\frac{dp}{dz}\right)_{fo} \varphi_{fo}^2; \varphi_{fo}^2 = (1-x)^2 + 2.87 x_e^2 p_r^{-1} + 1.54 Bd^{0.19} \left(\frac{\rho_f - \rho_g}{\rho_{tp}}\right)^{0.81}$ For $Bd Re_f^{0.5} > 200$, use HEM with Beattie & Whalley's [40] μ_{tp} relation	• Adiabatic flow • Fluid: R134a, R245fa, R236ea, R410a, R22, R404a, R12, R422d, R32, ammonia, propane, N_2 • Shape: circular and non-circular • Hydraulic diameter: 0.148–3.25 mm

Table 3
Summary of SFM-based empirical correlations for boiling and condensing flows.

Author(s) (Year)	Equation(s)	Database of Development
Qu & Mudawar (2003) [51]	$C = 21\left[1-\exp\left(-0.319\times10^{3}D_h\right)\right](0.00418G+0.0613)$	• Flow boiling • Fluid: water • Shape: non-circular • Hydraulic diameter: 348.9 μm
Lee & Mudawar (2005) [19]	$C = \begin{cases} 1.45Re_{fo}^{0.25}We_{fo}^{0.23}, & Re_f < 2000, Re_g \geq 2000(vt) \\ 2.16Re_{fo}^{0.047}We_{fo}^{0.60}, & Re_f < 2000, Re_g < 2000(vv) \end{cases}$	• Flow boiling • Fluid: R134a • Shape: non-circular (rectangular) • Hydraulic diameter: 713 μm height and 231 μm width
Kim & Mudawar (2013) [8]	$Re_{fo} = \frac{GD_h}{\mu_f},$ $C_{non-boiling} = \begin{cases} 0.39Re_{fo}^{0.03}Su_{go}^{0.10}(\rho_f/\rho_g)^{0.35}, & Re_f \geq 2000, Re_g \geq 2000(tt) \\ 8.7\times10^{-4}Re_{fo}^{0.17}Su_{go}^{0.50}(\rho_f/\rho_g)^{0.14}, & Re_f \geq 2000, Re_g < 2000(tv) \\ 0.0015Re_{fo}^{0.59}Su_{go}^{0.19}(\rho_f/\rho_g)^{0.36}, & Re_f < 2000, Re_g \geq 2000(vt) \\ 3.5\times10^{-5}Re_{fo}^{0.44}Su_{go}^{0.50}(\rho_f/\rho_g)^{0.48}, & Re_f < 2000, Re_g < 2000(vv) \end{cases}$ $C = \begin{cases} C_{non-boiling}\left[1+60We_{fo}^{0.32}\left(Bo\frac{P_h}{P_f}\right)^{0.78}\right], & Re_f \geq 2000 \\ C_{non-boiling}\left[1+530We_{fo}^{0.52}\left(Bo\frac{P_h}{P_f}\right)^{1.09}\right], & Re_f < 2000 \end{cases}$	• Flow boiling • Fluid: R134a, R12, R410A, R245fa, ammonia, FC72, CO_2, water • Shape: circular and non-circular • Hydraulic diameter: 0.349–5.35 mm
Jung & Radermacher (1989) [52]	$\left(\frac{dp}{dz}\right)_F = \left(\frac{dp}{dz}\right)_{fo}\varphi_{fo}^2; \varphi_{fo}^2 = 12.82X_{tt}^{-1.47}(1-x)^{1.8}$ $X_{tt} = \left(\frac{\mu_f}{\mu_g}\right)^{0.1}\left(\frac{1-x}{x}\right)^{0.9}\left(\frac{\rho_g}{\rho_f}\right)^{0.5}$	• Flow boiling • Fluids: R12, R22, R114, R152, their mixtures • Shape: circular • Diameter: 9.1 mm
Yan & Lin (1998) [53]	$\left(\frac{dp}{dz}\right)_F = -0.22\,Re_e^{-0.1}\frac{G^2}{D_h}\left[v_f + x\,v_{fg}\right]$	• Flow boiling • Fluid: R134a • Shape: circular • Diameter: 2.0 mm
Tran et al. (2000) [54]	$\left(\frac{dp}{dz}\right)_F = \left(\frac{dp}{dz}\right)_{fo}\varphi_{fo}^2;$ $\varphi_{fo}^2 = 1+\left[4.3\frac{(dp/dz)_{go}}{(dp/dz)_{fo}}-1\right]\left[N_{conf}x^{0.875}(1-x)^{0.875}+x^{1.75}\right]$	• Flow boiling • Fluids: R134a, R12, R113 • Shape: circular and non-circular • Diameter: 2.46 and 2.92 mm
Yu et al. (2002) [55]	$\left(\frac{dp}{dz}\right)_F = \left(\frac{dp}{dz}\right)_f\varphi_f^2; \varphi_f^2 = \left[18.65\left(\frac{v_f}{v_g}\right)^{0.5}\left(\frac{1-x}{x}\right)\frac{Re_g^{0.1}}{Re_f^{0.5}}\right]^{-1.9}$	• Flow boiling • Fluid: water • Shape: circular • Diameter: 2.98 mm
Sun & Mishima (2009) [56]	$\left(\frac{dp}{dz}\right)_F = \left(\frac{dp}{dz}\right)_f\varphi_f^2;$ For $Re_f < 2000$ and $Re_g < 2000$, $\varphi_f^2 = 1+\frac{C}{X}+\frac{1}{X^2}; C = 26\left(1+\frac{Re_f}{1000}\right)\left\{1-\exp\left(\frac{-0.153}{0.27\,N_{conf}+0.8}\right)\right\}$ For $Re_f \geq 2000$ or $Re_g \geq 2000$, $\varphi_f^2 = 1+\frac{C}{X^{1.19}}+\frac{1}{X^2}; C = 1.79\left(\frac{Re_g}{Re_f}\right)^{0.4}\left(\frac{1-x}{x}\right)^{0.5}$	• Boiling and adiabatic flow • Fluids: R123, R134a, R22, R236ea, R245fa, R404a, R407C, R410a, R507, CO_2, water-air • Shape: circular and non-circular • Hydraulic diameter: 0.506–12 mm
Ma et al. (2024) [57]	$\left(\frac{dp}{dz}\right)_F = \left(\frac{dp}{dz}\right)_f\varphi_f^2; \varphi_f^2 = \left[1+2690\left(\frac{Bd^{0.97}}{X_{tt}^{0.43}p_r^{0.95}}\right)\right]Re_f^{1.03}We_{fo}^{0.53}$ $X_{tt} = \left(\frac{1-x}{x}\right)^{0.9}\left(\frac{\rho_g}{\rho_f}\right)^{0.5}\left(\frac{\mu_f}{\mu_g}\right)^{0.1}$	• Boiling and condensing flow • Fluids: Water, R134a, CO_2, R236fa, R245fa, HFE 7100, R1234yf, R1233zd(E), R1234ze(E)¸acetone, R600a • Shape: circular and non-circular • Hydraulic diameter: 0.1–2.6 mm
Muradkhani et al. (2023) [17]	$\left.\frac{dp}{dz}F\right)_{tp} = \left.\frac{dp}{dz}\right)_f\left[1+\frac{C}{X}+\frac{1}{X^2}\right], \varphi_f^2 = 1+\frac{C}{X}+\frac{1}{X^2}X = \sqrt{\frac{\left.\frac{dp}{dz}\right)_f}{\left.\frac{dp}{dz}\right)_v}},$ $C = \begin{cases} 5.463(x)^{-0.081}(Re_{tp})^{-0.042}(Pr_{tp})^{-1.26}(P_{red})^{-1.11}(Bo)^{0.026}(R)^{-6.214}, For\,Bd \leq 3 \\ 1.02(x)^{-0.448}(Re_{tp})^{0.399}(Pr_{tp})^{-1.852}(P_{red})^{-0.329}(Bo)^{-0.753}(R)^{1.214}, For\,Bd > 3 \end{cases}$	• Boiling and condensing flow • Fluid: CO_2. • Shape: circular and non-circular • Hydraulic diameter: 0.1 — 7.72 mm
Nie et al. (2023) [16]	$\left.\frac{dp}{dz}F\right) = \left(\frac{dp}{dz}\right)_f\varphi_f^2 = \left(\frac{dp}{dz}\right)_g\varphi_g^2$ $\left(\frac{dp}{dz}F\right) = -\left(\frac{dp}{dz}\right)_g + C\left(\frac{dp}{dz}\right)_g^{\left(1-\frac{n}{2}\right)}\left(\frac{dp}{dz}\right)_f^{\frac{n}{2}} - \left(\frac{dp}{dz}\right)_f$ $\left(\frac{dp}{dz}\right)_f = \frac{2f_fG^2(1-x)^2}{\rho_fD}, \left(\frac{dp}{dz}\right)_g = \frac{2f_gG^2x^2}{\rho_gD}$ $\varphi_g^2 = 1+CX^n+X^2, X = \sqrt{\left(\frac{dp}{dz}\right)_f \Big/ \left(\frac{dp}{dz}\right)_g}$	• Boiling, condensing, and adiabatic flow • Fluid: Ethanol, methane, nitrogen, R123, R1234yf, R1234ze(E), R1270, R134a, R14, R152a, R22, R245fa, R290, R32, R402A, R404A, R407C, R410A, R452B, R455A, R502, R600a, R601, R717, R744 • Shape: circular and non-circular • Hydraulic diameter: 0.24 — 14.45 mm

(*continued on next page*)

Table 3 (*continued*)

Author(s) (Year)	Equation(s)	Database of Development
	$C = \begin{cases} 0.94Fr_{tp}^{0.26}x^{-0.4}Bd^{0.05}J_v^{-0.35}, n = 0.55, J_v = \frac{Gx}{[gD\rho_g(\rho_f - \rho_g)]^{0.5}}, \text{Annular Flow} \\ Co^{0.47} + 0.291Fr_{tp}^{0.55}Bd^{0.13}J_v^{-0.72}, n = 0.73, \text{Non} - \text{Annular Flow} \end{cases}$ $Co = \left(\frac{1}{x-1}\right)^{0.8}\left(\frac{\rho_g}{\rho_f}\right)^{0.5}, Fr_{tp} = \frac{G^2}{g\rho_{tp}^2 D},$ $\rho_{tp} = \left[\frac{x}{\rho_g} + \frac{1-x}{\rho_f}\right]^{-1}$ $J_v = \frac{Gx}{[gD\rho_g(\rho_f - \rho_g)]^{0.5}}$ Based on Cavallini et al. (2002) $J_v = \begin{cases} \geq 2.5 \quad G > G_w, \text{Annular Flow} \\ < 2.5 \; or \; G \leq G_w, \text{Non} - \text{Annular Flow} \\ G_w = \text{Mass} - \text{flux threshold} = \rho_f(gD)^{0.5}\left(0.54 - 0.96Bd^{-2} - 4.2Bd^{-1}\right) \end{cases}$	

Non-circular: rectangular, square, triangular.

database covers mass velocities from 99 to 2000 kg.m^{-2}.s, tube diameter from 0.5 to 14.0 mm, reduced pressure from 0.0363 to 0.6896 and pressure gradient from 0.3 to 1332 kPa.m^{-1}. In this improved model, they introduced an interfacial friction enhancement factor by correlating liquid-to vapor core inertia-force ratio and reduced pressure. The proposed model predicted the database with MAE of 18.16%.

These models provide stronger physical insight compared to empirical correlations. However, they are generally more complex than HEM and SFM approaches, are often developed for specific flow regimes, and require multiple closure relations. For these reasons, despite their strong physical foundation, their direct application as universal predictive tools remains limited.

3. Consolidated database

3.1. Database for single circular mini/micro-channels

2882 data points for saturated flow boiling in mini/micro-channels are collected from 19 studies spanning 13 working fluids. Of these, 2528 data points are obtained from 16 studies for horizontal orientation and 354 data points from 3 studies on vertical upflow orientation. The collected database is for smooth channels only, and channels with surface enhancements are excluded. The database was assembled with the objective of incorporating as many relevant studies as possible on smooth circular and non-circular channels under saturated flow boiling conditions. Inclusion was based on the availability of complete information required to evaluate the governing dimensionless groups and the frictional pressure gradient. Studies, or specific data points, that exhibited significant deviation from the overall trends of the consolidated database were carefully examined and, where justified, excluded. Only one study by Zhu et al. [67], which investigated the flow boiling of R32, showed substantial deviation from the rest of the dataset. This study was poorly predicted by all evaluated correlations, with MAE values as high as 142%. The large discrepancy appears to stem from the highly specialized nature of the study, which encompassed a wide range of flow regimes, including stratified, slug, churn, annular, dryout, and mist flows. In contrast, the present work focuses on the assessment and development of a generalized correlation applicable across a broad consolidated database. Therefore, only this study was completely excluded from the correlation development process. As a result, the final database represents a comprehensive yet carefully screened global dataset, rather than a uniformly distributed dataset across the entire operating space.

Table 4 summarizes the key characteristics of each dataset, including fluid, hydraulic diameter, mass flux, and orientation. The amassed database spans:

- **Fluids:** Ammonia, CO_2, R12, R32, R134a, R410A, R1270, R245fa, R1234yf, R1234ze (E), R152a, R600a, and water.
- **Hydraulic diameter:** $D_h = 0.529$–8 mm.
- **Mass flux**: $G = 33$–2738 kg/(m^2.s).
- **Liquid-only Reynolds number:** $Re_{fo} = 352$–27,984.
- **Quality:** $0 < x < 1$.
- **Reduced pressure:** $p_r = 0.038$–0.47.
- **Bond number:** $Bd = 0.24$–75.

These broad ranges enable thorough evaluation of predictive methods across different fluids and operating conditions.

The distribution of the database is presented in Fig. 2. Fig. 2(a) illustrates the distribution of data points across the working fluids included in the dataset. The database is primarily dominated by CO_2, R134a, and R1234ze(E), contributing 27.5%, 19.7%, and 16% of the total dataset, respectively. Moderate contributions are observed from R1234yf (9.5%) and Ammonia (8%). The least represented fluids include R1270, R32, R410A, R600a, and R152a, each contributing less than 2% of the dataset. Overall, the database encompasses a wide range of fluids with diverse thermophysical properties, including both conventional and low-GWP refrigerants.

Fig. 2(b) presents the distribution of the dataset with respect to mass flux (G). The database spans a broad range of mass flux values from 33 to 2738 kg/(m^2.s), covering both low and high flow regimes. Approximately 61.3% of the data points fall below 500 kg/(m^2.s), while 31% lie within the range of 500–900 kg/(m^2.s). The remaining ~8% of the data corresponds to mass flux values exceeding 900 kg/(m^2.s).

Fig. 2(c) shows the distribution of the data points with respect to the channel diameter. Majority (~83.79%) of the database is concentrated between the channel diameter of 0 to 3 mm. About 14.54% of the data is between 3 and 5 mm. The remaining small fraction ~1.67% of the data is between 5 and 8 mm.

Fig. 2(d) shows the histogram of the experimental frictional pressure gradient. Approximately 3.5% of the data points fall below 10^3 Pa·m^{-1}, while the majority (84.5%) lie within the range of 10^3–10^5 Pa·m^{-1}. The remaining 12% of the dataset corresponds to frictional pressure gradients exceeding 10^5 Pa·m^{-1}.

3.2. Database for single non-circular mini/micro-channels

591 data points for saturated flow boiling in single non-circular (square and rectangular) mini/micro-channels are collected from 5 studies covering 8 fluids. Of these, 475 and 116 data points are for horizontal and vertical orientations, respectively. The database spans mass velocities of $G = 100$–1400 kg/(m^2.s), mini/micro-channel hydraulic diameters of $D_h = 0.68$–5.35 mm and qualities of $0 < x < 1$. Table 5 shows the list of studies included in the database.

The distribution of the database is presented in Fig. 3. Fig. 3(a) illustrates the distribution of data points across the working fluids included in the dataset. The largest contribution is from R410A, accounting for 28% of the total database. The second and third largest contributions are from R22 and FC-72, representing 23% and 20% of the dataset, respectively. Newer low-GWP fluids, including R454C, R454B, R1234yf, and R32, collectively contribute approximately 15% of the database. Fig. 3(b) shows the distribution of the dataset with respect to mass flux (G). Approximately 55% of the data lies below 500 kg/(m^2.s), which is representative of moderate mass flux applications. About 18% of the data falls within the range of 500–600 kg/(m^2.s), while approximately 25% spans the range of 600–1500 kg/(m^2.s). Only 11 data points (1.8%) are available for mass flux values exceeding 1500 kg/(m^2.s), indicating limited high-mass-flux coverage.

Fig. 3(c) shows the distribution of database with respect to hydraulic diameter. The majority of the data, ~72%, corresponds to the channel hydraulic diameter below 4 mm. The channels of hydraulic diameter 3 to 4 mm represents about 43% of the database. The remaining data are distributed over diameters up to 5.5 mm.

Fig. 3(d) presents the distribution of the frictional pressure gradient. The histogram reveals a broad, non-normal distribution spanning approximately 10^3 to 10^6 Pa·m^{-1}. Most data points are concentrated in the ranges of 10^3–10^5 Pa·m^{-1}, with a secondary cluster observed between 10^5 and 10^6 Pa·m^{-1}. This multimodal behavior indicates substantial variability within the dataset.

Note that surface-enhanced channels are excluded to maintain uniformity. For instance, Huh and Kim's [90] data for boiling flow in a single coated channel are not included in this database. Some studies were excluded due to key operating information not having been reported. These are the studies of: (i) Azarhazin et al. [91] on single non-circular channels being excluded due to missing heat flux and inlet condition information, (ii) Soupremanien [92] on Forane 365 HX being excluded due to subcooled conditions of the experiment, (iii) Qin et al. [93], Candan et al. [94] and Markal et al. [95] on water in single rectangular channels being excluded due to missing inlet condition information. Excluded studies are listed in Table 6.

4. Predictive performance of existing pressure drop correlations for saturated flow boiling

The predictive performance of selected seminal correlations and models is evaluated using the consolidated database. Although a wide range of historical correlations exists in the literature, only a representative subset is considered in the present study. In particular, emphasis is placed on the classical Lockhart–Martinelli method and C-type formulations, which form the basis for comparison with the proposed correlation. The performance of each correlation is quantified using standard statistical metrics, including mean absolute error (MAE), root mean square error (RMSE), mean bias error (MBE), and the coefficient of determination (R^2), defined as follows:

$$MAE = \frac{1}{N}\sum \frac{\left|\left(\frac{dp}{dz}\right)_{f,\exp} - \left(\frac{dp}{dz}\right)_{f,pred}\right|}{\left(\frac{dp}{dz}\right)_{f,\exp}} \times 100\% \tag{19}$$

$$RMS = \sqrt{\frac{1}{N}\sum \left[\frac{\left(\frac{dp}{dz}\right)_{f,\exp} - \left(\frac{dp}{dz}\right)_{f,pred}}{\left(\frac{dp}{dz}\right)_{f,\exp}}\right]^2} \times 100\% \tag{20}$$

$$MBE = \frac{1}{N}\sum \left[\frac{\left(\frac{dp}{dz}\right)_{f,\exp} - \left(\frac{dp}{dz}\right)_{f,pred}}{\left(\frac{dp}{dz}\right)_{f,\exp}}\right] \times 100\% \tag{21}$$

$$R^2 = 1 - \frac{\sum\left(\left(\frac{dp}{dz}\right)_{f,\exp} - \left(\frac{dp}{dz}\right)_{f,pred}\right)^2}{\sum\left(\left(\frac{dp}{dz}\right)_{f,\exp,mean} - \left(\frac{dp}{dz}\right)_{f,pred}\right)^2} \tag{22}$$

4.1. Assessment of HEM-based mixture viscosity models over dataset for circular channels

Fig. 4 shows parity plots of the prediction assessment of HEM-based mixture viscosity models over 2882 circular mini/micro-channel frictional pressure gradient data points.

Fig. 4(a) reveals Owens' [38] model predicts the circular dataset with a MAE of 25.41% and 62% of data points within ±50% error. This model treats the two-phase mixture as fully dominated by the liquid and equates mixture viscosity to pure liquid viscosity meaning it completely ignores vapor viscosity. The good accuracy indicates that the effects of the vapor phase are negligible compared to liquid, validating Owens' hypothesis for this database.

Fig. 4(b) shows the model by Cicchitti et al. [37] predicts the circular dataset with a MAE of 33.33%. It underpredicts the majority of data points for R12, CO_2, and R1234yf, which is because of two reasons.

Table 4
Frictional pressure drop data for single circular mini/micro-channels collected from the literature.

Study	Fluid	D_h [mm]	G [kg/(m^2.s)]	Data points	Orientation
Lezzi (1994) [68]	Water	1	776–2738	86	H
Tran (1998) [69]	R12, R134a	2.46	33–832	413	H
Huo (2005) [70]	R134a	2.01,4.26	400–500	74	VU
Owahib et al. (2008) [71]	R134a	0.826,1.224,1.7	100–400	51	VU
Hu et al. (2009) [72]	R410A	2,4.18	200–620	48	H
Ducoulombier (2010) [73]	CO_2	0.529	400–1200	268	H
Tibirica & Ribatski (2011) [74]	R245fa	2.32	199–701	142	H
Tibirica et al. (2011) [75]	R134a	2.32	100–600	49	H
Wu et al. (2011) [76]	CO_2	1.42	300–600	254	H
Maqbool et al. (2012) [77]	Ammonia	1.224,1.7	100–500	229	VU
Qiu et al. (2015) [78]	R1234ze(E)	8	200–400	48	H
Longo et al. (2016) [79]	R134a, R1234ze (E)	4	200–600	176	H
Pabon et al. (2019) [80]	R1234yf	4.8	300	22	H
Zhang et al. (2020) [81]	CO_2	1.5	300–600	273	H
Xu et al. (2021) [82]	R1234ze (E)	1.88	540–870	321	H
Xu et al. (2022) [83]	R1234yf	1.88	540–870	252	H
Mudhafar and Pan (2022) [84]	R32	4	200–600	37	H
Oliveria et al. (2023) [85]	R1270	1	320	17	H
Longo et al. (2024) [86]	R600a,R152a,R134a	4	150–400	122	H

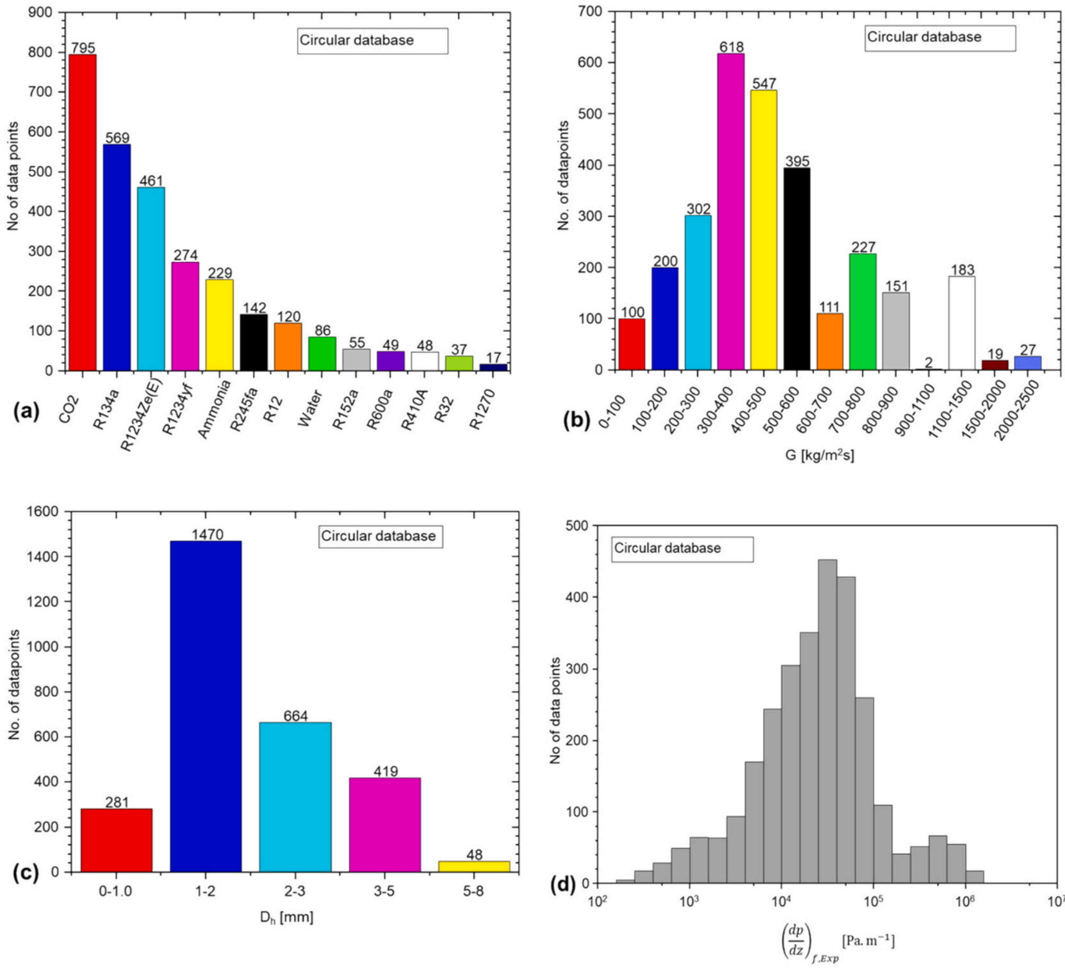

Fig. 2. Distribution of the database: (a) data points by fluid, (b) data points by mass flux range, (c) data points by channel diameter, (d) histogram of experimental frictional pressure gradient.

Firstly, it is developed only for water over a narrow operating range, and large errors are expected when used for other fluids and outside the bounds of the original database for water. Secondly, the underprediction also worsens at higher pressure gradient values which means that the assumption of homogenous flow does not hold at higher x as during boiling in mini/micro-channels where flow is predominantly separated.

Fig. 4(c) shows the model of Lin et al. [41] largely underpredicts R12, R245fa, CO_2, and ammonia data with a MAE of 45.92%. Although this correlation was developed for small tubes of 0.66 and 1.17 mm diameter, it is inaccurate for the following reasons: (i) it was developed only using 238 data points for R-12 vaporization and lacks generalization, (ii) it was developed for a quality range of 0–0.25 meaning that it does not work for higher quality because at higher quality due to flow separation this relation cannot capture the boiling flows in mini/micro-channels, (iii) their experiments were conducted only for the horizontal orientation, and (iv) the authors claiming the effect of mass flux was negligible for their database, which is not true for the present database.

Fig. 4(d) shows that the model proposed by Beattie and Whalley [40] significantly underpredicts the majority of the data, yielding an MAE of 45.95%. The large scatter indicates that the implicit treatment of flow-pattern effects through the viscosity formulation is insufficient to capture the influence of surface tension and interfacial structures in boiling flows. Moreover, the model was originally developed for adiabatic round-tube flows and does not include a momentum source term to account for vapor generation. Consequently, it cannot be reliably generalized to boiling or condensing flows and exhibits limited applicability to saturated boiling in mini- and micro-channels.

Fig. 4(e) shows that the correlation proposed by McAdams et al. [34] also underpredicts most of the data, with an MAE of 49.33%. This behavior can be attributed to three primary factors. First, similar to other HEM-based relations, it assumes a uniformly mixed flow, which becomes invalid in boiling conditions due to phase separation at higher vapor qualities. Second, the model does not include the influence of surface tension or confinement. The present database has confinement

Table 5
Frictional pressure drop data on single non-circular mini/micro-channels collected from the literature.

Study	Fluid	D_h [mm]	G [kg/(m^2.s)]	Data points	Orientation
Quiben et al. (2009) [87]	R22,R410A	3.71,4.88,5.35	150–500	261	H
Kharangate et al. (2012) [44]	FC72	3.3	177–1652	116	VU
Kim et al. (2013) [88]	R410A	3,4.4	200–400	44	H
Keepaiboon et al. (2016) [12]	R134a	0.68	600–1400	80	H
Li et al. (2025) [89]	R454C, R454B, R1234yf,R32	2.857	100–200	90	H

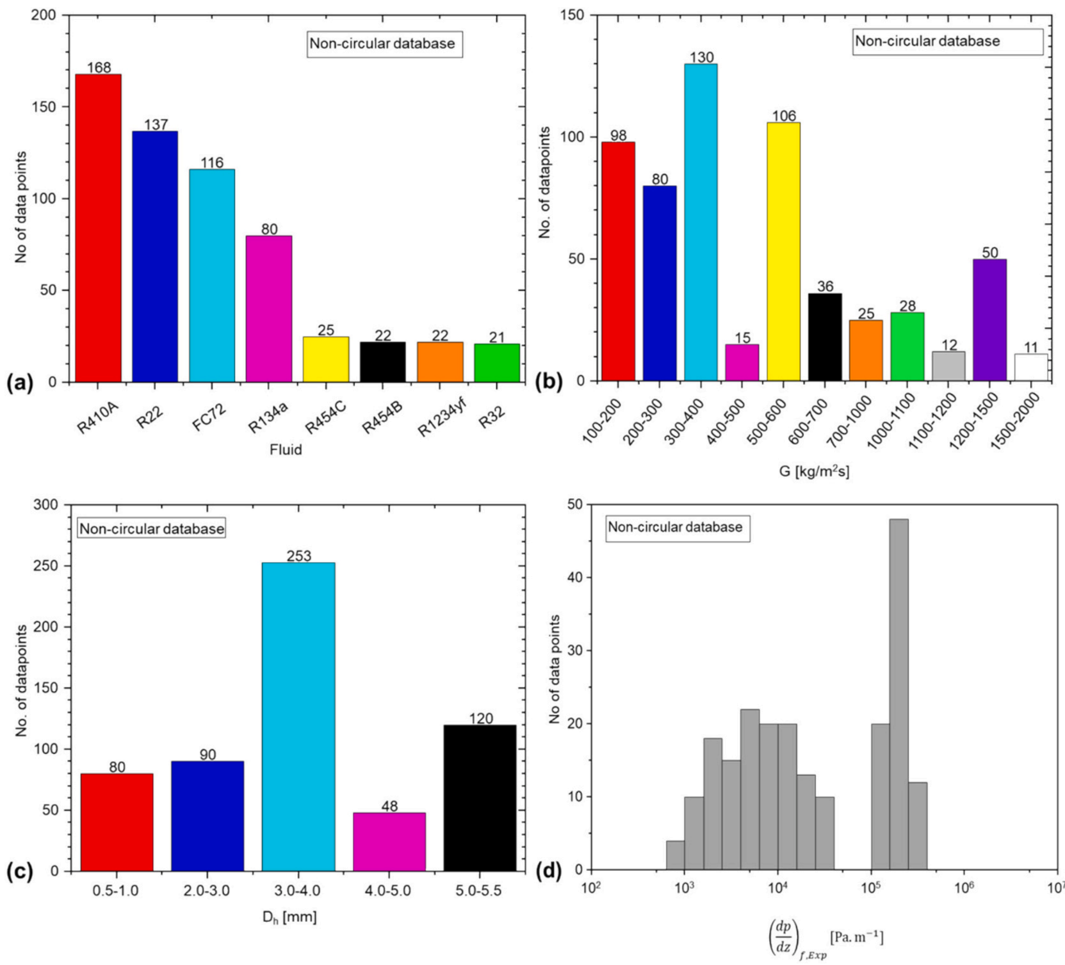

Fig. 3. Distribution of the database: (a) data points by fluid, (b) data points by mass flux range, (c) data points by hydraulic diameter, (d) histogram of experimental frictional pressure gradient.

number ranging from 0.11 to 2.03 indicating that surface tension and gravity effects varies significantly across the database. Since this model has no parameter to capture these variations in mini/micro-channels, it cannot consistently predict well. Third, the correlation was originally developed using a benzene–oil mixture database and is therefore not directly applicable to a wide range of fluids with varying thermophysical properties.

Fig. 4(f) reveals the relation by Akers et al. [36] predicts with a MAE of 50.75%, mainly underpredicting for CO_2, R12, R245fa, ammonia, and R1234yf. The reasons is that it was developed using data for (i) larger diameter tubes having $N_{conf} \sim 0.048–0.477$ while present database lies in the confined flow regime ($N_{conf} \sim 0.11–2.03$) where surface tension has a strong influence on the phase distribution and (ii) condensing flows (not boiling flows), reinforcing Kim and Mudawar's [8] hypothesis that flow boiling data should be treated separately from adiabatic/condensing flow data. Overall, condensation-driven viscosity models does not work well for boiling flows.

Fig. 4(g) shows the relation of Dukler et al. [39] underpredicts majority of the data with an overall MAE of 52.19% due to the following reasons. Firstly, this relation is based on volumetric average of liquid and vapor viscosities. Since, $v_g >> v_f$, the predicted μ_{tp} can become biased towards gas viscosities as the quality increases, leading to inaccurate Reynolds number and friction factor estimates. Secondly, the relation was derived using 2650 adiabatic flow data points for air-water, natural gas, and oil in large tubes, and fails to predict boiling flows.

Fig. 4(h) reveals the relation by Davidson et al. [35] yields large overpredictions and a 216.65% MAE. This trend is opposite to that of previous relations which underpredicted the majority of the data. The large overpredictions is because of the fact that this relation was derived from steam-water data in tubes of 12.5–44.5 mm diameter, making it suitable only for large diameter tubes.

Overall, Fig. 4 shows that HEM based mixture viscosity models are less reliable for predicting frictional pressure gradient for mini/micro-channels. This is because boiling flows in mini/micro-channels involve slip between the liquid and vapor phases and significant interfacial shear which are not adequately captured by HEM based formulations. Therefore, a more robust model should include parameters that represent surface tension, inertia, density and viscosity differences.

Table 6
Studies on single non-circular mini/micro-channels excluded from the present database.

Study	Refrigerant	Reason
Huh & Kim (2007) [90]	Water	Enhanced micro-channel
Soupremanien (2011) [92]	Forane 365 HX	Subcooled flow boiling
Qin et al. (2012) [93]	Water	Insufficient inlet information such as x_{in}
Candan et al. (2018) [94]	Water	Insufficient inlet information such as p_{inlet}
Markal et al. (2018) [95]	Water	Insufficient inlet information such as p_{inlet}
Azarhazin et al. (2020) [91]	R1234yf	Missing heat flux and inlet condition information

4.2. Assessment of SFM-based correlations over dataset for circular channels

Parity plots showing the predictive performance of SFM-based semi-empirical correlations over the single circular mini/micro-channel dataset are included in Fig.5. Fig. 5(a) shows the recently reported universal correlation by Nie et al. [16] predicts the data with a MAE of 23.42%, the lowest among all correlations in this study. It underpredicts 15.8% of the R134a and 7% of the CO_2 data below −50% error bound. The good performance of this correlation is attributed to its broad database which also includes confined flows as correlation covers the channels of hydraulic diameter varying between 0.24 and 14.45 mm.

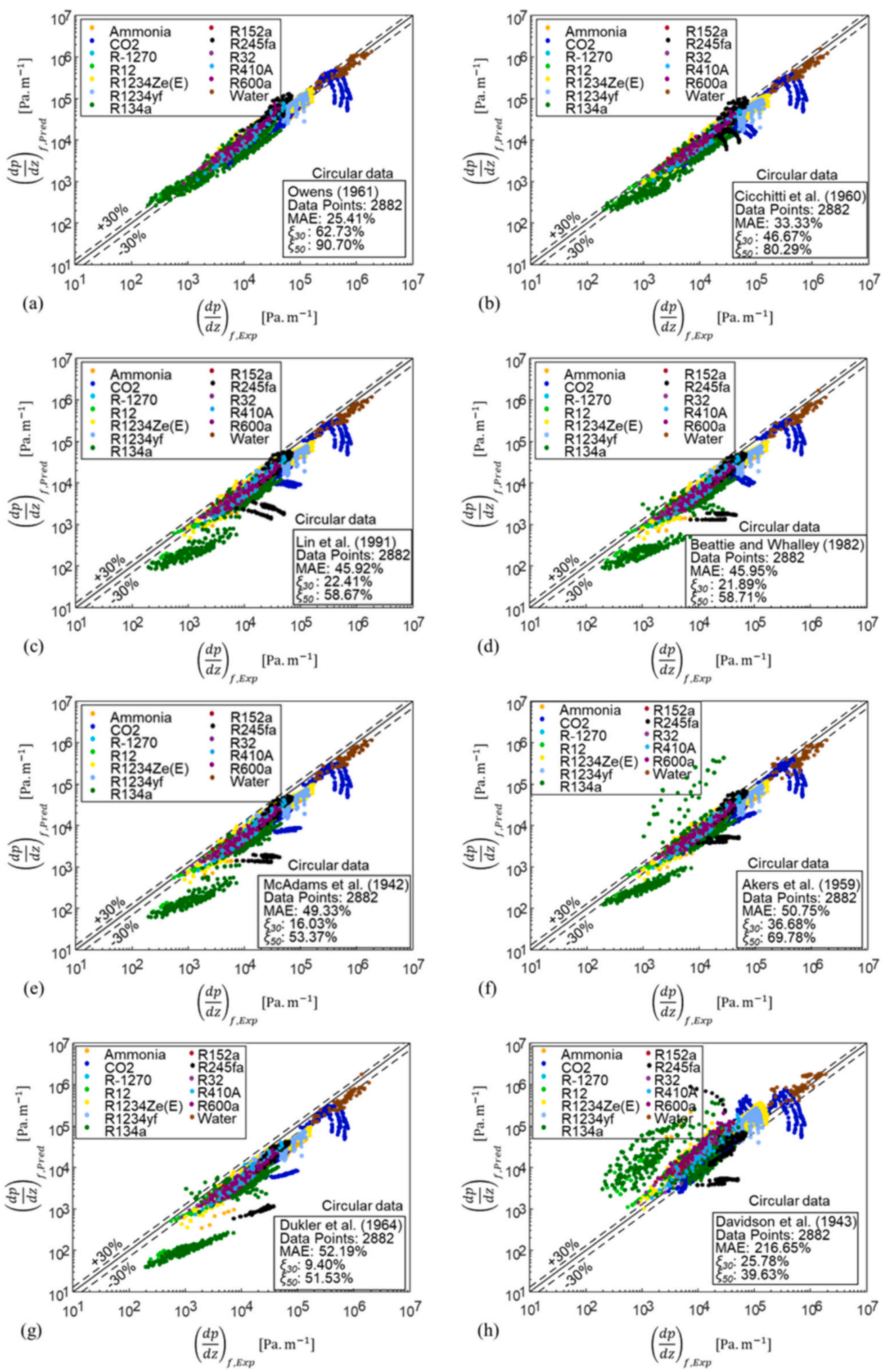

Fig. 4. Parity plots assessing the predictive performance of HEM-based mixture viscosity models for saturated flow boiling frictional pressure gradient of circular mini/microchannels: (a) Owens' [38], (b) Cicchitti et al. [37], (c) Lin et al. [41], (d) Beattie and Whalley (1982) [40], (e) McAdams et al. (1942) [34], (f) Akers et al. (1959) [36], (g) Dukler et al. (1964) [39] and (h) Davidson et al. (1943) [35].

Fig. 5(b) shows Kim and Mudawar's [8] universal correlation predicts well for most of the data, with the MAE of 24.93%. This is expected because their correlation was developed for mini/microchannels and includes the influence of surface tension and density ratio which are physically relevant to the current database. However, it overpredicts R1234yf, R32 and R1234ze(E), data is partially overpredicted beyond +50% error bound by 43%, 32.4%, 31.6% respectively. This is due to the fact that these refrigerants were not used for developing their correlation, and these fluids introduced different density ratio, viscosity ratio, and reduce pressures which potentially alter interfacial shear and vapor-liquid momentum exchange. Therefore, including newly reported data for these fluids is a straight-forward way to improve its accuracy.

Fig. 5(c) shows Mishima and Hibiki's [45] correlation predicted the third best with a MAE of 27.6%. This correlation expresses the Chisholm parameter C as a function of D_h. Its reasonable performance reflects the importance of the channel size and confinement in the mini/micro-channel flows. However, it also overpredicts 35% of the R1234ze(E) data beyond ±50% error bound. This is not surprising since the correlation does not explicitly include boiling flow specific effects such as quality variation or heat flux effect. Therefore, while D_h is an important parameter, it alone is not sufficient to represent the combined influence of inertia, surface tension and other phase-change effects in boiling flows in mini/micro-channels.

Fig. 5(d) shows the correlation by Moradkhani et al. [17] predicts the circular database with MAE of 44.12%. This correlation failed to capture the physical trends in the data because it was developed only for CO_2 and cannot be generalized for refrigerants. Since the present database contains fluids with a broad range of thermophysical properties which strongly influence slip ratio and interfacial shear, a correlation developed for a single fluid cannot be expected to generalize well.

Fig. 5(e) shows that the correlation proposed by Qu and Mudawar [51] predicts the dataset with an MAE of 53.63%, significantly overpredicting most of the data, including that for water. This discrepancy can be attributed to several factors. First, the correlation was specifically developed for the flow boiling of water, limiting its general applicability to other working fluids. Second, the underlying database corresponds primarily to laminar–laminar flow conditions, restricting its validity across different flow regimes. Third, the formulation incorporates only diameter and mass flux as governing parameters, neglecting other critical factors such as fluid properties, interfacial effects, and phase distribution.

Fig. 5(f) shows Lockhart and Martinelli's [9] correlation predicts with a MAE of 53.65%. Although this correlation remains one of the most widely used SFM-based approaches, it was originally developed for adiabatic flows in relatively large circular tubes using water, oil, Kerosene, and benzene. It predicts 91% and 80% of R245fa and R134a data, respectively, within error margin of ±50% and overpredicts 81%, 52%, 51%, and 39% of the data beyond the +50% margin for R32, R1234yf, R1234ze(E) and CO_2, respectively. This shows that macroscale adiabatic flow correlations cannot fully capture the interfacial and confinement controlled physics of boiling flows in mini/micro-channels.

Fig. 5(g) shows Lee and Lee's [46] correlation exhibits a MAE of 71.62% with 100%, 82%, and 79% of R32, R1234yf, and R1234ze(E), respectively, the data being over predicted above error margin of +50%. This overprediction is largely because of two reasons. Firstly, this correlation was developed using a database for air-water adiabatic flow in which phase distribution and interfacial structure are governed primarily by gas and liquid flow rates. In boiling flows, however, vapor is continuously generated along the heated length causing axial acceleration and quality changes. These effects are not represented in this correlation formulation; therefore, it fails to capture interfacial behavior during boiling flows in mini/micro-channels. Secondly, due to the significant difference in phase densities and thermophysical properties, this correlation does not apply to other fluids.

Finally, Fig. 5(h) shows Lee and Mudawar's [19] correlation predicted with a MAE of 72.93%. Even though it was proposed for flow boiling, it suffers from a lack of universality, being derived only using a dataset of R134a flow boiling in a rectangular channel.

Overall, the results in Fig. 5 demonstrate that correlations capturing mini/micro-channel effects such as confinement and surface tension perform better than classical adiabatic flow correlations. This observation confirms that there is a need for a new correlation that accounts for both fluid-property effects and channel-scale effects when predicting boiling flows frictional pressure gradient in mini/micro-channels.

4.3. Assessment of HEM-based mixture viscosity models over dataset for non-circular channels

Fig. 6 shows the prediction performance of HEM-based mixture viscosity models for the single non-circular mini/micro-channel dataset.

Fig. 6(a) shows that the correlation proposed by Cicchitti et al. [37] predicts the dataset with an overall MAE of 32.66%. The model fails to accurately predict data from one side heated studies involving FC-72 and R134a, and also underpredicts portions of the R410A dataset. This behavior can be attributed to two primary reasons. First, HEM-based correlations are generally valid only when the flow is well mixed, whereas flow in mini- and micro-channels is predominantly separated. Second, when only one side or three sides are heated, vapor generation becomes non-uniform and the liquid film gets redistributed asymmetrically along the heated and unheated walls, making the assumption of a uniformly mixed flow invalid, thereby limiting the applicability of HEM formulations.

Fig. 6(b) shows that the correlation proposed by Akers et al. [36] yields an MAE of 35.22%, while also failing to predict data for FC-72, R134a, and R410A. Like other HEM models, this model is also based on an effective mixture viscosity and assumes two-phase behaves as a pseudo-single phase. This assumption becomes questionable in non-circular mini/micro-channels, where large vapor-liquid density difference and confinement promote phase separation. For the present database, liquid to vapor density ratio varies between 23 and 84 with average of 46.18 and viscosity ratio varies between 10 and 31, with average of 17.43, indicating strong differences in liquid and vapor momentum transport. These huge differences promote slip and interfacial shear which are not directly captured by this formulation leading towards discrepancies in predictions.

Fig. 6(c) shows that Owens [38] predicts the dataset with an overall MAE of 36.11%. Notably, the model underpredicts approximately 25% of the data for FC-72 flow boiling in a single-side-heated rectangular channel beyond the ±50% error bounds. This underprediction is due to the fact that this model is unable to account for asymmetric vapor generation in partially heated channels. Since HEM models use a cross sectionally averaged mixture viscosity, they cannot identify these differences, therefore predicts poorly.

Fig. 6(d) shows that the correlation proposed by Lin et al. [41] predicts with an MAE of 39.99%, underpredicting approximately 24%, 29%, and 47% of the data for R410A, R134a, and FC-72, respectively, outside the ±50% error bounds. This discrepancy is attributed to the fact that in non-circular channels local shear substantially differ from those assumed in HEM models. Therefore, HEM based models cannot capture. Fig. 6(e) shows that the correlation proposed by McAdams et al. [34] predicts 37.23% of the data within a ± 30% error band, with an overall MAE of 40.01%. This model treats two-phase viscosity using quality weighted form, but it does not include the influence of surface tension, confinement or non-circular geometry. The present database has confinement number ranging from 0.16 to 1.24 indicating that surface tension and gravity effects varies significantly across the database. Since this model has no parameter to capture these variations, it cannot consistently predict well.

Fig. 6(f) shows that the relation by Beattie and Whalley [40] predicts the dataset with an MAE of 40.55%, while underpredicting approximately 23%, 49%, and 29% of the R410A, FC-72, and R134a data points, respectively, outside the ±50% error bounds. This model does not

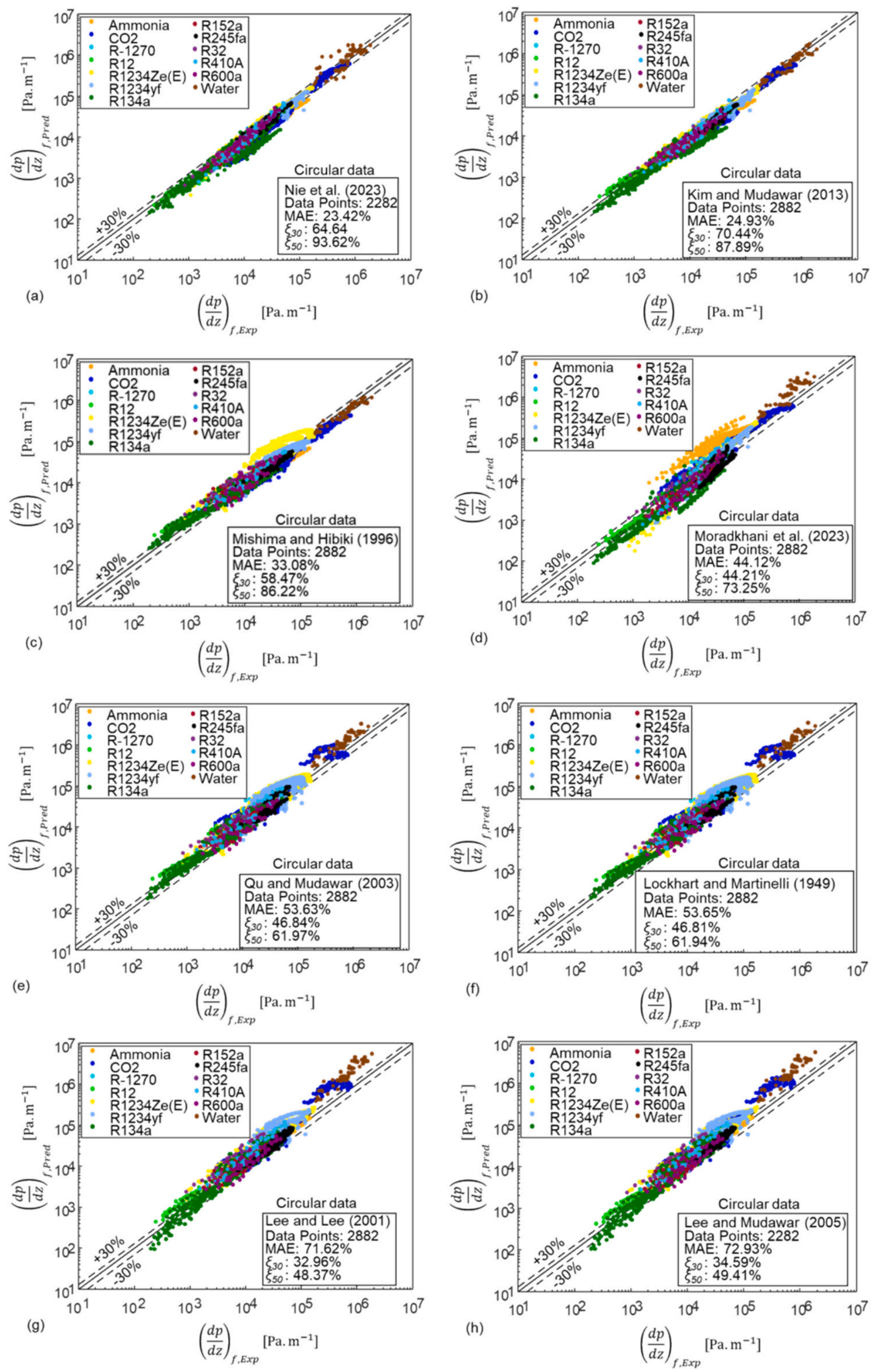

Fig. 5. Parity plots assessing the predictive performance of SFM-based semi-empirical correlations for saturated flow boiling frictional pressure gradient of circular mini/microchannels: (a) Nie et al. (2023) [16], (b) Kim and Mudawar (2013) [8], (c) Mishima and Hibiki (1996) [45], (d) Moradkhani et al. (2023) [17], (e) Qu and Mudawar (2003) [51], (f) Lockhart & Martinelli (1949) [9], (g) Lee and Lee (2001) [46], and (h) Lee and Mudawar (2005) [19].

capture the influence of surface tension and phase separated interfacial structures in boiling flows in mini/micro-channels. Consequently, it cannot be generalized to boiling flows.

Fig. 6(g) shows that the correlation proposed by Dukler et al. [39] predicts only 24.37% of the data within ±30% error bounds, with an overall MAE of 46.84%, indicating poor predictive capability for flow boiling in non-circular channels. Its poor prediction can be attributed to its formulation which can produce unrealistic values due to the high specific volume ratio between liquid and vapor. This issue become more severe for fluids with large density differences where small changes in quality can cause large changes in vapor volumetric fraction. Since the model does not include confinement or geometry effects, it is not suitable for generalized prediction for boiling flows in mini/micro-channels. Additionally, this correlation was originally developed for adiabatic air–water, natural gas, and oil flows in large-diameter tubes, and therefore does not adequately capture the physics of boiling flows in mini- and micro-channels.

Fig. 6(h) shows that the relation proposed by Davidson et al. [35] performs the worst among all evaluated models, predicting only 11.84% of the data within ±30% error bounds and yielding the highest MAE of 239.95%. Although this model is also based on HEM, it consistently overpredicts the present dataset. This behavior is primarily attributed to

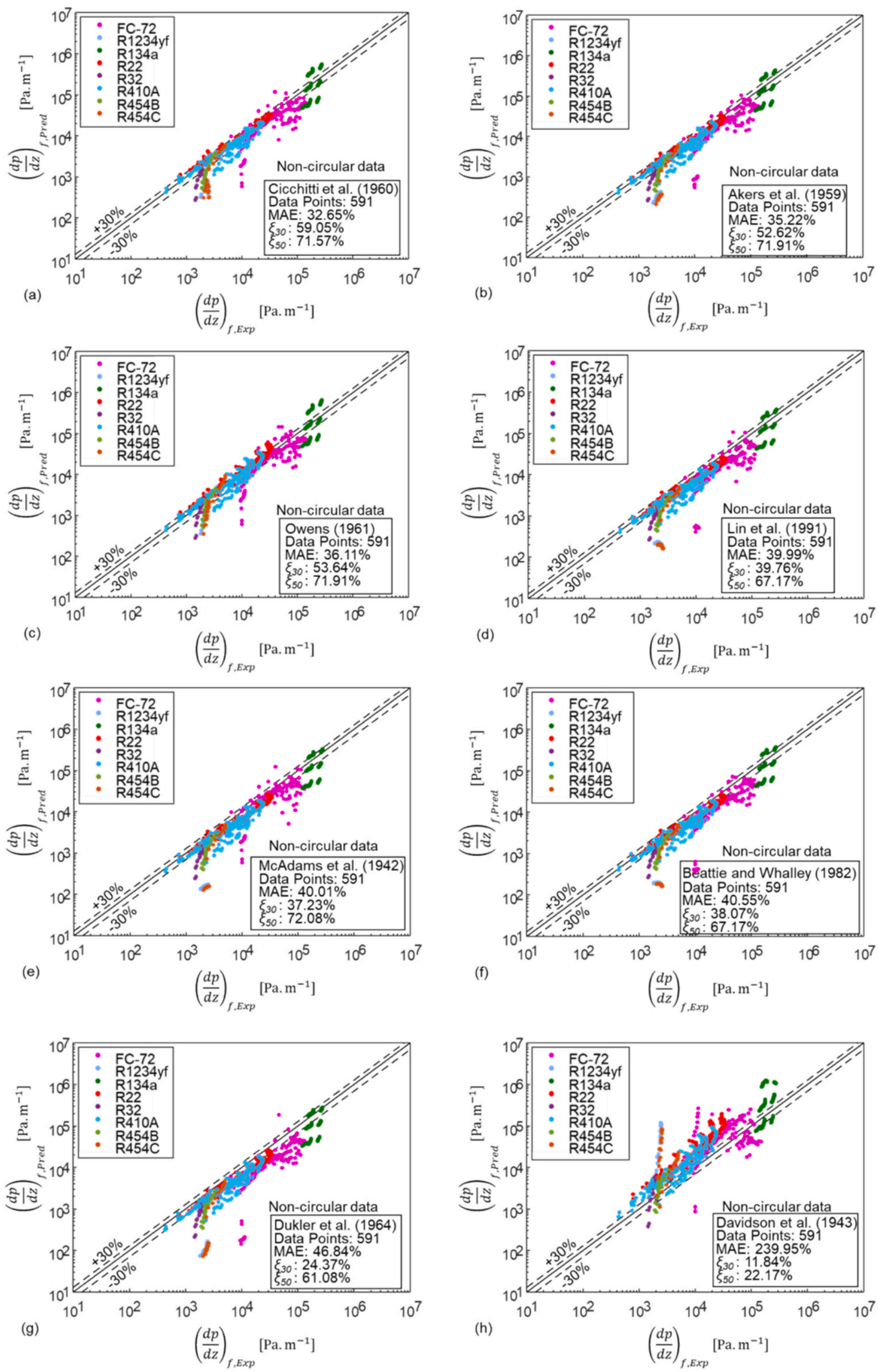

Fig. 6. Parity plots assessing the predictive performance of HEM-based mixture viscosity models for saturated flow boiling frictional pressure gradient of non-circular mini/microchannels database: (a) Cicchitti et al. (1960) [37], (b) Akers et al. (1959) [36], (c) Owens (1961) [38], (d) Lin et al. (1991) [41], (e) McAdams et al. (1942) [34], (f) Beattie & Whalley (1982) [40], (g) Dukler et al. (1964) [39] and (h) Davidson et al. (1943) [35].

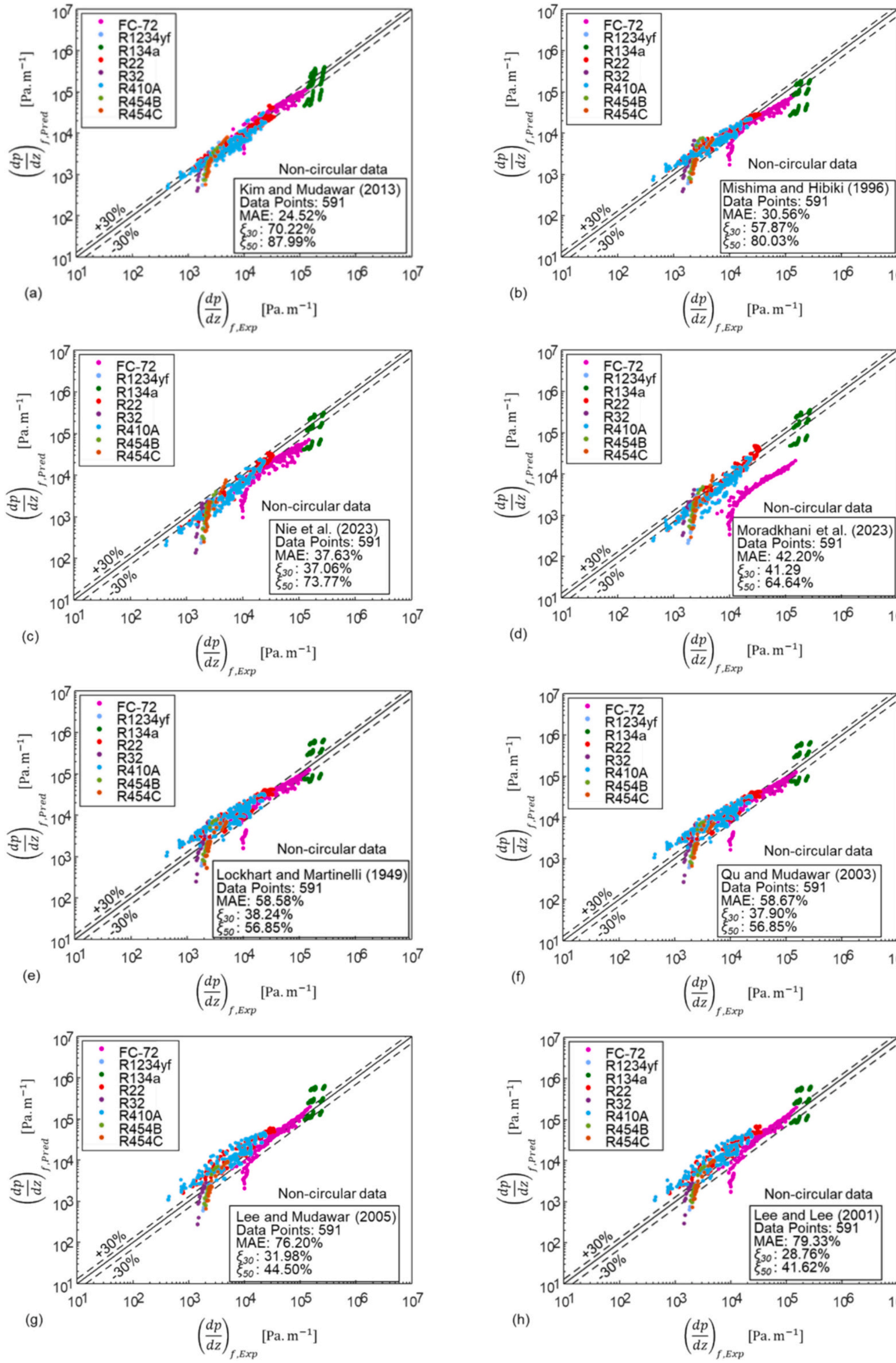

Fig. 7. Parity plots assessing the predictive performance of SFM-based semi-empirical correlations for saturated flow boiling frictional pressure gradient of non-circular mini/microchannels: (a) Kim and Mudawar (2013) [8], (b) Mishima and Hibiki (1996) [45], (c) Nie et al. (2023) [16], (d) Moradkhani et al. (2023) [17], (e) Lockhart and Martinelli (1949) [9], (f) Qu and Mudawar (2003) [51], (g) Lee and Mudawar (2005) [19], and (h) Lee and Lee (2001) [46].

its two-phase viscosity formulation, which can produce unrealistically large values even at moderate vapor qualities due to the high specific-volume ratio between vapor and liquid phases. Furthermore, the model was originally developed for steam–water flow in large tubes (12.5–44.5 mm diameter), making it unsuitable for application to mini- and micro-channel boiling flows.

Overall, Fig. 6 shows that HEM based mixture viscosity models are less reliable for mini/microchannels. The reason is that mini/micro-channels involves slip between two-phases, asymmetric heating effects, and interfacial shear, all of which are not adequately represented in

Table 7
Error Matrix of seminal models/correlations for pressure drop of saturated flow boiling.

Model/ Correlation	Circular (2882 data points)				Non-circular (rectangular and square) (591 data points)				Overall, MAE (%)
	HEM Based								
	MAE	RMS	MBE	R^2	MAE	RMS	MBE	R^2	
McAdams et al. (1942)	49.33	53.45	49.20	0.72	40.01	47.32	34.89	0.69	47.74
Davidson et al. (1943)	216.65	648.29	−205.39	0.49	239.95	562.86	−229	−9.06	220.62
Akers et al. (1959)	50.75	152.41	24.97	0.72	35.22	43.46	25.36	0.62	48.10
Cicchitti et al. (1960)	33.33	38.9	28.74	0.76	32.65	44.04	14.87	0.38	33.21
Owens (1961)	25.41	31.85	11.42	0.81	36.11	48.54	−2	0.11	27.23
Dukler et al. (1964)	52.19	55.69	51.76	0.70	46.84	53.53	44.42	0.66	51.27
Beattie & Whalley (1982)	45.95	50.53	45.13	0.72	40.55	47.11	34.22	0.66	45.03
Lin et al. (1991)	45.92	50.45	45.36	0.73	39.99	47	33.10	0.66	44.91
Awad & Muzychka (2008)	38.32	42.08	37.71	0.75	43.23	46.71	37.36	0.66	39.15
	SFM Based								
Lockhart & Martinelli (1949)	53.65	74.91	−40.98	0.22	58.58	80.20	−41.76	−0.99	54.89
Mishima & Hibiki (1996)	33.08	46.19	−1.15	0.89	30.56	40.38	6.27	0.64	32.65
Lee & Lee (2001)	71.62	97.89	−67.28	−2.9	79.33	105	−68.8	−0.57	72.93
Qu & Mudawar (2003)	53.63	74.90	−40.94	0.23	58.67	80.30	−42.15	−0.99	54.48
Lee & Mudawar (2005)	72.93	100.5	−68.47	−3.01	76.20	102.18	−65.50	−0.54	73.49
Kim & Mudawar (2013)	24.93	33.41	−8.6	0.89	24.52	30.70	5.26	0.75	24.86
Zeng et al. (2021)	62.74	72.27	50.29	0.46	66.32	69.77	62	0.66	63.35
Moradkhani et al. (2023)	44.12	65.06	−11.24	0.05	42.20	50.50	32.28	0.62	43.79
Nie et al. (2023)	23.42	29.67	16.37	0.9	37.63	42.50	33.13	0.73	25.83
New Correlation	**19.22**	**24.33**	**3.49**	**0.98**	**23.13**	**28.87**	**4.30**	**0.81**	**19.88**

HEM based models. Therefore, it is necessary to have a framework that includes parameters representing surface tension, inertia, density ratio, viscosity ratio, and geometry.

4.4. Assessment of SFM-based correlations over dataset for non-circular channels

Parity plots showing the predictive performance of SFM-based semi-empirical correlations over the non-circular single mini/micro-channel dataset (both uniformly and non-uniformly heated) are included in Fig. 7.

Fig. 7(a) shows the Kim and Mudawar's correlation [8] predicts the entire dataset with a MAE of 24.52%, the lowest among all evaluated correlations. This indicates that the correlation has relatively good universality for non-circular mini/micro-channel boiling flows. Its better performance is due to the inclusion of surface tension, inertia, heat flux, and density ratio effects through dimensionless groups such as Suratman number, Weber number, Boiling number, and liquid to vapor density ratio. These parameters are crucial in confined boiling flows where the frictional pressure gradient is governed not only by wall friction but also by liquid-vapor momentum exchange and interfacial shear. However, there are some deviations since this correlation does not explicitly include non-circular geometry effects such as aspect ratio.

Fig. 7(b) shows Mishima and Hibiki's correlation [45] predicts 57.87% of the data within ±30% error with an overall MAE of 30.56%.

Table 8
Comparison between Kim and Mudawar [8] and new correlation.

Component	Kim and Mudawar (2013)	New Correlation
Flow regime-classification	Reynolds-number states of the liquid and vapor phases	Same classification retained
$C_{non\text{-}boiling}$	Piecewise $C_{non\text{-}boiling}$ correlation for *tt,tv,vt*, and *vv* regime	Coefficient refitted using expanded database
$C_{boiling}$	$1 + d\, We_{fo}^{e}\left(Bo\frac{P_h}{P_f}\right)^f$	$1 + d\, We_{fo}^{e}\left(Bo\frac{P_h}{P_f}\right)^f \beta^g Pr_{tp}^h$ To incorporate geometric and thermo-physical influence β and Pr_{tp} were added.

Although originally developed for adiabatic two-phase flows, this correlation exhibit reasonable performance because it includes D_h dependent Chisholm relation and distinguishes between circular and non-circular channels. However, it fails to predict the FC-72 and R134a data points. One possible reason is these two sets of data points are for one-sided and three sided heated mini/micro-channels, where asymmetric vapor generation changes the liquid-film distribution and interfacial shear which the correlation does not account for.

Fig. 7(c) shows the recently reported universal correlation of Nie et al. [16] predicts with an overall MAE of 37.63%, with severe underpredictions of 52% of FC-72 and 29% of R134a data points in a one side heated and three side heated micro-channels. This suggest that asymmetric heating caused complexity which is not captured by this correlation.

Fig. 7(d) shows the correlation of Moradkhani et al. [17] only predicts 42.20% of the data within an error margin of ±30%. The overall performance seems reasonable because it was particularly derived using a CO_2 database. It underpredict all the FC-72 and 29% of the R134a data in one side and three side heated mini/micro-channels and this asymmetric heating is not accounted in the correlation. Additionally, since CO_2 has thermophysical properties substantially different from refrigerants, the correlation cannot be generalized to all fluids.

Fig. 7(e) shows Lockhart and Martinelli's correlation [9] predicts only 34% of the data within a ± 30% error bound and an overall MAE of 58.58%. It overpredicts the majority of the dataset, excepting 8% of data points near $dp/dz|_{f,exp} = 10$ kPa/m, while underpredicting 18% of R134a data points near $dp/dz|_{f,exp} = 150 - 250$ kPa/m. This poor performance is expected since the correlation was developed for adiabatic two-phase flow in relatively large channels and does not include confinement and boiling induced vapor generation or non-circular asymmetric heating effects. Therefore, it cannot adequately represent vapor-core/liquid-film structures and geometry dependent interfacial shear present in non-circular mini/micro-channels.

Fig. 7(f) shows Qu and Mudawar's correlation [51] predicts the data with a MAE of 58.67%. The overpredictions are because this correlation was derived from a single study on flow boiling of R134a in a rectangular micro-channel which only covered two flow regimes (laminar liquid and laminar vapor). This confirms that even correlation developed for microchannels may not be universal if they do not cover a broad range of D_h, N_{conf}, phase densities and heating configurations. Fig. 7(g)

Table 9
New universal correlation developed using the amassed global database.

$$C = \begin{cases} C_{non-boiling}\left[1 + 60.388\, We_{fo}^{1.4512}\left(Bo\dfrac{P_h}{P_f}\right)^{1.6685}\beta^{-1.1853}Pr_{tp}^{-0.2946}\right], & \mathrm{Re}_f \geq 2000 \\ C_{non-boiling}\left[1 + 530 We_{fo}^{0.1547}\left(Bo\dfrac{P_h}{P_f}\right)^{1.2682}\beta^{-0.2338}Pr_{tp}^{1.4988}\right], & \mathrm{Re}_f < 2000 \end{cases} \quad (28)$$

$$C_{non-boiling} = \begin{cases} 0.5073\mathrm{Re}_{fo}^{-0.1808}Su_{go}^{0.2429}\left(\rho_f/\rho_g\right)^{0.2159}, & \mathrm{Re}_f \geq 2000, \mathrm{Re}_g \geq 2000(tt) \\ 1.6858\times10^{-3}\mathrm{Re}_{fo}^{-0.0707}Su_{go}^{0.6133}\left(\rho_f/\rho_g\right)^{0.0737}, & \mathrm{Re}_f \geq 2000, \mathrm{Re}_g < 2000(tv) \\ 0.003889\mathrm{Re}_{fo}^{0.5632}Su_{go}^{0.1403}\left(\rho_f/\rho_g\right)^{0.3896}, & \mathrm{Re}_f < 2000, \mathrm{Re}_g \geq 2000(vt) \\ 9.3\times10^{-6}\mathrm{Re}_{fo}^{0.6796}Su_{go}^{0.5199}\left(\rho_f/\rho_g\right)^{0.3975}, & \mathrm{Re}_f < 2000, \mathrm{Re}_g < 2000(vv) \end{cases} \quad (29)$$

shows Lee and Mudawar's correlation [96] yielded the second highest MAE of 76.20%. This correlation is developed using a single study of flow boiling of R134a in a rectangular channel. Therefore, although the correlation is relevant to boiling flows in micro-channels, it lacks universality since it does not cover the wide range of hydraulic diameters, aspect ratios, and heating configurations. Its large error indicates that correlations developed from a single fluid and single geometry database do not generalize well to the universal database.

Fig. 7(h) shows Lee and Lee's [46] correlation yields the highest MAE of 79.33% among all evaluated correlations by predicting only 28.76% of the dataset within ±30% error margin, meaning it overpredicted ~71.24% of the data. The larger error is because it was derived only using air-water adiabatic flow data. In adiabatic flow, the phase distribution is determined by applied gas and liquid flow rates, whereas in boiling flows, vapor is continuously generated along the heated length. This causes axial quality variations, vapor acceleration, liquid-film thinning, and changes in interfacial shear. These boiling flow specific effects are absent in this correlation, leading to poor prediction of the present database of boiling flows.

Overall, Fig. 7 reveals that SFM-based correlations perform better than HEM-based mixture viscosity models, but their accuracy still depends on whether they account for boiling-specific and geometry specific effects. The wide range of D_h, N_{conf}, We_f, phase density ratios and heating configurations indicate that the database include different boiling regimes. Therefore, correlations derived using adiabatic flow, single fluids or limited geometries cannot provide universal predictions. Thus, there is a need to develop a universal framework which effectively captures the boiling flows physics in mini/micro-channels.

5. New universal correlation for two-phase frictional pressure drop

Among the 18 correlations evaluated, the correlation proposed by Kim and Mudawar [8] provided the best overall predictive performance across the consolidated database, as summarized in Table 7. Therefore, the present study adopts the classical Lockhart–Martinelli [9] framework as the basis for developing the proposed correlation, wherein the parameter C is reformulated in terms of relevant dimensionless groups. The dimensionless parameters commonly employed in two-phase flow correlations include Reynolds number, Weber number, Froude number, Bond number, confinement number, Suratman number, and density ratio. However, for mini- and micro-channel flows, the influence of body forces is negligible; therefore, the Froude number and Bond number are not considered [97]. Based on the literature survey and amassed database, following parameters are included in the correlation.

The first parameter is the liquid only Reynolds number which is incorporated to capture the interaction between inertial and viscous forces which influence wall shear and therefore frictional pressure

Table 10
Predictive performance of the two best existing and new correlations on individual datasets.

Dataset	Fluid	D_h [mm]	Mean Absolute Error (%)		
			Kim & Mudawar (2013)	Nie et al. (2023)	New correlation
Single circular channels					
Lezzi (1994) [68]	Water	1	15.60	35.48	8.44
Tran (1998) [69]	R12, R134a	2.46	20.00	42.91	22.48
Huo (2005) [70]	R134a	2.01,4.26	20.20	63.13	35.66
Owahib et al. (2008) [71]	R134a	0.826,1.224,1.7	19.85	33.87	19.75
Hu et al. (2009) [72]	R410A	2,4.18	15.20	22.03	17.27
Ducoulombier (2010) [73]	CO_2	0.529	13.40	12.24	11.74
Tibirica & Ribatski (2011) [74]	R245fa	2.32	7.90	11.08	9.33
Tibirica et al. (2011) [75]	R134a	2.32	12.30	37.30	21.55
Wu et al. (2011) [76]	CO_2	1.42	19.00	34.07	22.85
Maqbool et al. (2012) [77]	Ammonia	1.224,1.7	17.10	28.40	19.92
Qiu et al. (2015) [78]	R1234ze(E)	8	26.22	25.16	20.74
Longo et al. (2016) [79]	R134a, R1234ze (E)	4	18.34	34.13	22.34
Pabon et al. (2019) [80]	R1234yf	4.8	22.93	42.48	30.39
Zhang et al. (2020) [81]	CO_2	1.5	21.11	41.65	25.4
Xu et al. (2021) [82]	R1234ze(E)	1.88	40.54	8.94	14.61
Xu et al. (2022) [83]	R1234yf	1.88	52.99	10.08	16.31
Mudhafar & Pan (2022) [84]	R32	4	41.21	13.48	29.16
Oliveria et al. (2023) [85]	R1270	1	29.82	13.32	20.57
Longo et al. (2024) [86]	R600a, R152a, R134a	4	19.35	18.61	16.97
Single non-circular (rectangular and square) channels					
Quiben et al. (2009) [87]	R22, R410A	3.71,4.88,5.35	15.50	28.22	20.84
Kharangate et al. (2012) [44]	FC72	3.3	20.20	51.16	14.53
Kim et al. (2013) [88]	R410A	3,4.4	32.19	48.34	32.51
Keepaiboon et al. (2016) [12]	R134a	0.68	41.00	40.00	22.41
Li et al. (2025) [89]	R454C, R454B, R1234yf, R32	2.857	27.31	40.94	27.12

gradient. This is defined as:

$$\mathrm{Re}_{fo} = \frac{GD_h}{\mu_f} \tag{23}$$

The second parameter is vapor-only Suratman number, which is included to account for relative influence of surface tension and viscous effects. It combines surface tension, hydraulic diameter of the channel, vapor density, and therefore it helps in capturing the interfacial effects in small channels. It can be computed as:

$$\mathrm{Su}_{go} = \frac{\sigma\rho_g D_h}{\mu_g^2} \tag{24}$$

The third parameter is liquid to vapor density ratio which is included to account for the large density difference between the two-phases. Since density ratio influences vapor velocity, slip between two-phases, and therefore the interfacial shear, it directly affects the frictional pressure gradient. Moreover, in the present database, the density ratio varies widely from 9.49 to 167, making its incorporation necessary for a generalized correlation across different fluids.

The forth parameter is liquid-only Weber number which is included to account for the balance between inertial and surface tension forces. Its inclusion is necessary for mini/micro-channels flow boiling since role of surface tension becomes more prominent in small diameter channels. It is defined as:

$$We_{fo} = \frac{G^2 D_h}{\sigma\rho_f} \tag{25}$$

The fifth parameter is Boiling number (Bo). This parameter is included to account for the influence of wall heat flux on the two-phase flow such as rate of vapor production, quality variation, and liquid-film during the flow boiling. It is defined as:

$$Bo = \frac{q''}{Gh_{fg}} \tag{26}$$

In addition, the ratio of heated perimeter to wetted perimeter (P_h/P_f) is added as a multiplier to account for the effect of non-uniformly heated channels.

The sixth parameter is aspect ratio (β) of the channels. This is introduced to account for the geometric effects. It is defined as $\beta = 1$ for circular channels and ratio of the shorter to the longer side for non-circular channels. Since channel shape affects liquid-film distribution and wall/interfacial shear, β helps extend the correlation to both circular and non-circular geometries.

The seventh parameter included in this correlation is two-phase Prandtl number. It is introduced to incorporate the Viscous–thermal transport effects and can be computed as:

$$Pr_{tp} = xPr_g + (1-x)Pr_f \tag{27}$$

Using these dimensionless groups, a new correlation is developed that predicts the entire database with the lowest MAE among the evaluated models. The coefficients of the proposed correlation are determined via nonlinear regression by directly minimizing the MAE between predicted and experimental frictional pressure gradients. The optimization is performed using the BFGS algorithm (Broyden–-Fletcher–Goldfarb–Shanno) method, with the original Kim and Mudawar's coefficient [8] used as initial estimates for the non-boiling term, and physically reasonable initial guesses employed for the remaining parameters. The optimization is carried out simultaneously over the full database until convergence of the objective function is achieved. By incorporating these additional dimensionless parameters, the proposed correlation improves predictive accuracy for newer refrigerants while maintaining robust performance across conventional fluids. A comparison between the Kim and Mudawar correlation and the proposed formulation is provided in Table 8. The new correlations for C are provided in Table 9 which needs to be used in Eq. (12) given above in Section 2.1. Table 10 contains the predictions of the new correlation on each individual dataset. The new correlation performed well on all datasets including new refrigerants. It predicts the R1234yf dataset reported by Xu et al. [83] with a MAE of 16.31%, a major improvement over Kim and Mudawar's [8] universal correlation, which inadequately predicted the same dataset with a 52.99% MAE. Similarly, the new correlation also predicts Xu et al.'s (2021) R1234ze(E) data with MAE of 14.61% which is also a significant improvement as compared to the Kim and Mudawar's [8] which predicted it with MAE of 40.54%. The new correlation has also improved the prediction accuracy on the R32 study reported by Mudhafar and Pan (2022) [84] as it predicts all the data with MAE of 29.61% as compared to 41.21% prediction MAE of Kim and Mudawar's [8]. Of all individual studies, the new correlation exhibits the highest MAE of 35.4% on Huo's data [70], which is 15% higher than the original Kim and Mudawar correlation [8]. This small tradeoff is made to accurately predict the new refrigerants which were very poorly predicted by Kim and Mudawar's correlation [8].

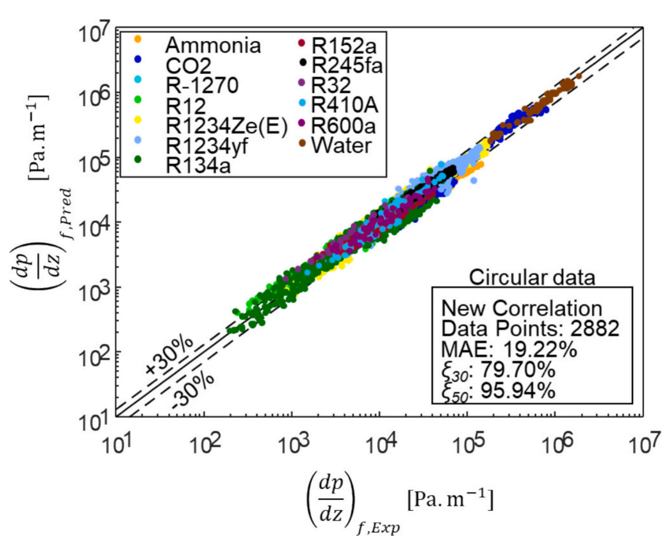

Fig. 8. Predictions by the new correlation on the circular mini/micro-channel database.

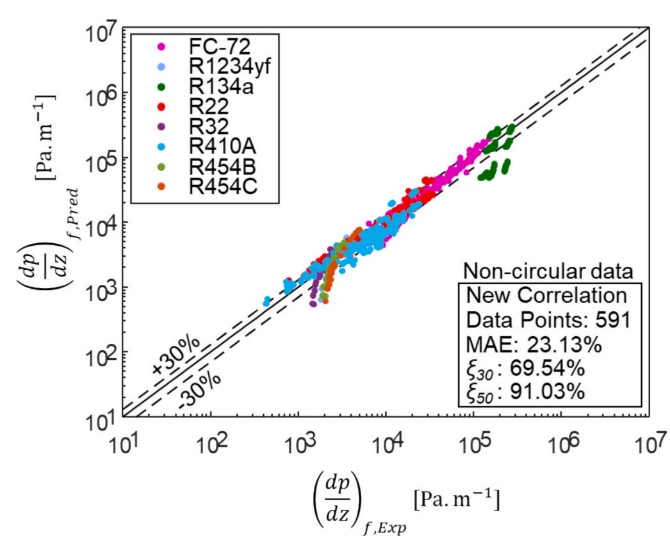

Fig. 9. Prediction by new correlation on the non-circular mini/micro-channel database.

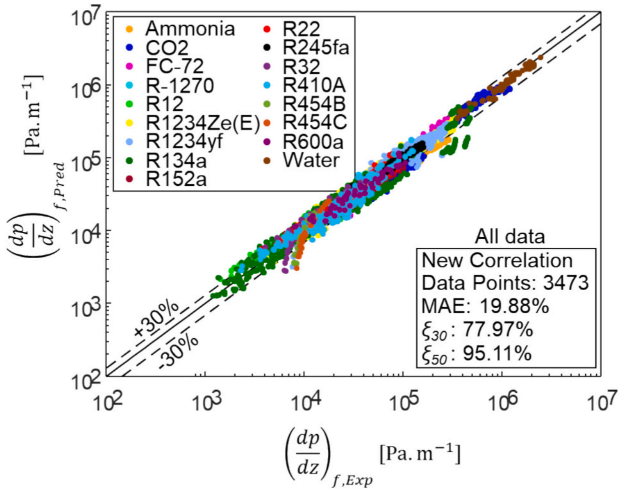

Fig. 10. Prediction by the new correlation on all the consolidated database.

5.1. Predictions of new correlation for single circular mini/micro-channels

The new correlation predicts all the circular single channel data points with a MAE of 19.22%, as shown in Fig. 8. Although ~4% of data points are still overpredicted outside the ±50% error margin, it predicts most new refrigerants, including R32, R1234ze(E), and R1234yf with far better accuracy, making it a superior choice for predicting the pressure gradient of new low-GWP refrigerants.

5.2. Predictions of new correlation for single non-circular mini/micro-channels

The new correlation predicts all the non-circular single channel data points with a MAE of 23.13%, as shown in Fig. 9. This is higher than the circular channel predictions probably due to the lack of large dataset for single non-circular channels and skewing of the entire database towards circular channels. However, it improved the predictive accuracy of the previously best performing correlation [8] by about 1.4%.

The overall performance of the new correlation on all the database is shown below in Fig.10. The correlation predicts all the data with a MAE of 19.88%. Approximately 78% of the data is predicted within error margin of ±30% and 95% of the data is predicted within error bound of ±50%.

Fig. 11 shows the predictive performance of the new correlation, reported in Table 9, for each individual flow regime. The correlation predicts the data with MAEs of 29.64, 20.05, 14, and 19.76% for the laminar liquid-laminar vapor (*vv*), laminar liquid-turbulent vapor (*vt*),

Table 11
Validity range of the proposed correlation.

Parameter	Range
G [kg/(m^2.s)]	33–2738
x	0–1
D_h [mm]	0.529–8
p_{red}	0.038–0.47
q' [w/m^2]	2.15–2363
Fluid	Ammonia, CO₂, R12, R22, R410A, FC72, R134a, R454C, R454B, R1234yf, R32, R1270, R245fa, R1234ze (E), R152a, R600a, and water.

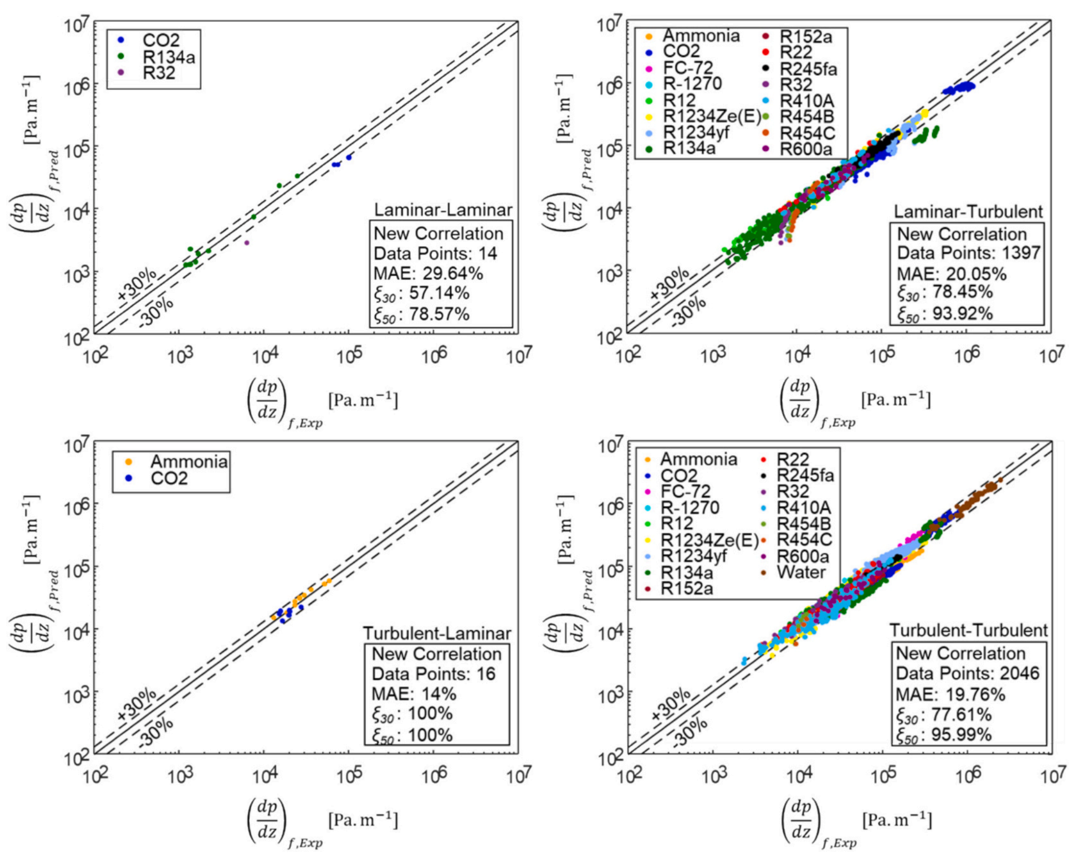

Fig. 11. Prediction Performance of new correlation on the entire consolidated database for: (a) laminar liquid-laminar vapor, (b) laminar liquid-turbulent vapor, (c) turbulent liquid-laminar vapor, and (d) turbulent liquid-turbulent vapor.

turbulent liquid-laminar vapor (*tv*) and turbulent liquid-turbulent vapor (*tt*) flow regimes respectively, showing the uniformly good predictive performance across all regimes of the entire database. Of all four regimes, the *vv* dataset has the highest MAE, possibly because it contains the fewest data points (14); the accuracy can be improved by incorporating more data points, however, this regime has the least practical interest given the low flow velocities.

5.3. Engineering implications of the new correlation

The proposed correlation has direct relevance to the design and optimization of compact two-phase systems. In MCHXs, accurate prediction of frictional pressure gradient is crucial for estimating total pressure drop, pumping power and refrigerant distribution. In HVAC systems, pressure drop significantly influences evaporator performance and overall system efficiency. The incorporation of both circular and non-circular channels makes the correlation applicable to practical multiport tubes and compact MCHXs. The correlation is also applicable for high-heat flux electronics cooling applications where flow boiling mini/micro channels is used to remove high heat loads. Excessive pressure drop in such kind of systems also leads towards increase in power requirement. Therefore, it is necessary to evaluate selected geometry, channel dimensions, and operating conditions before performing detailed experimentation, which the present correlation can support. The validity range of the proposed correlation is listed in Table 11.

6. Conclusions

This study assesses the performance of existing two-phase frictional pressure gradient correlations for saturated flow boiling of single circular and non-circular mini/micro-channels. The best performing correlations have been identified and further improved for better prediction over a wide range of fluids and operating conditions. Key conclusions are as follows:

(i) HEM-based mixture viscosity models showed an average MAE of 69.44%, while SFM-based correlations showed an average MAE of 46.59%.

(ii) Of all existing correlations, Kim and Mudawar's [8] correlation was found to be the most accurate, with a MAE of 24.86%.

(iii) To evaluate the accelerational pressure-gradient component, Zivi void fraction correlation [43] was employed within the SFM framework. This selection is supported by prior assessments demonstrating that Zivi's correlation provides reliable predictions compared to other slip-based void fraction models [8]. The accelerational component was subsequently subtracted from the total pressure gradient to isolate the frictional pressure gradient. It is necessary to subtract these losses before evaluating the frictional pressure gradient correlations because in some cases these losses can be non-negligible. For instance, in Kharangate et al. (2012) [44] study on the one-sided heated upflow boiling of FC-72 in a 2.5 × 5 mm rectangular channel, the accelerational pressure gradient accounts for 17 to 36% of the total pressure gradient. The gravitational pressure gradient contribution ranges from 4.77% to 62.72% with an average of 16.96%. On the other hand, in the Keepaiboon et al. (2016) [12] study on the boiling flow of R134a in micro-channel under horizontal orientation, the accelerational pressure gradient contribution varied between ~1 to 12% because of the shorter heated length and other operating conditions.

(iv) A new universal correlation was developed by improving Kim and Mudawar's correlation [8] by incorporating the geometrical and fluid thermophysical property parameters. It predicts the entire database with an overall MAE of 19.88%.

(v) The literature lacks sufficient studies on single non-circular mini/micro-channels. Further research is needed to fill the gap, particularly for new low-GWP refrigerants.

(vi) Future research may focus on extending the present framework to multiport channels, where flow maldistribution can lead to significant pressure losses. Additionally, further refinement through flow-pattern-based approaches or physics-assisted and uncertainty-aware machine learning frameworks may enhance predictive capability and generalizability.

Declaration of competing interest

The authors declare the following financial interests/personal relationships which may be considered as potential competing interests: The co-authors from Carrier Corporation are Carrier employees. The other co-authors have no known financial interests or personal relationships that could have appeared to influence the work reported in this paper.

Acknowledgement

The authors appreciate the support of the Carrier corporation.

Data availability

The data that has been used is confidential.

References

[1] I. Mudawar, Assessment of high-heat-flux thermal management schemes, IEEE Trans. Compon. Packag. Technol. 24 (2001) 122–141, https://doi.org/10.1109/6144.926375.

[2] I. Mudawar, S.J. Darges, V.S. Devahdhanush, M.M. Hasan, H.K. Nahra, R. Balasubramaniam, J.R. Mackey, Pressure drop characteristics and prediction techniques (models/correlations and artificial neural networks) for microgravity flow boiling onboard the international Space Station, Int. J. Heat Mass Transf. 240 (2025) 126593, https://doi.org/10.1016/j.ijheatmasstransfer.2024.126593.

[3] S. Mehdi, Y. Shah, N.-H. Kim, Bubble dynamics of R-123 and R-134a on pore/sub-tunnel surfaces, Int. J. Therm. Sci. 177 (2022) 107543, https://doi.org/10.1016/j.ijthermalsci.2022.107543.

[4] M. Visaria, I. Mudawar, Application of two-phase spray cooling for thermal management of electronic devices, IEEE Trans. Compon. Packag. Technol. 32 (2009) 784–793, https://doi.org/10.1109/TCAPT.2008.2010405.

[5] N. Damle, I. Mudawar, J. Hartwig, Liquid nitrogen spray characterization in ambient and development of correlations for droplet diameter and velocity, Thermal Sci. Eng. Progress 69 (2026), https://doi.org/10.1016/j.tsep.2025.104384.

[6] V.S. Devahdhanush, I. Mudawar, Review of critical heat flux (CHF) in jet impingement boiling, Int. J. Heat Mass Transf. 169 (2021), https://doi.org/10.1016/j.ijheatmasstransfer.2020.120893.

[7] S.-M. Kim, I. Mudawar, Review of databases and predictive methods for heat transfer in condensing and boiling mini/micro-channel flows, Int. J. Heat Mass Transf. 77 (2014) 627–652.

[8] S.M. Kim, I. Mudawar, Universal approach to predicting two-phase frictional pressure drop for mini/micro-channel saturated flow boiling, Int. J. Heat Mass Transf. 58 (2013) 718–734, https://doi.org/10.1016/j.ijheatmasstransfer.2012.11.045.

[9] R.W. Lockhart, R.C. Martinelli, Proposed correlation of data for isothermal two-phase, two-component flow in pipes, Chem. Eng. Prog. 45 (1949) 39–48.

[10] L. Friedel, Improved friction pressure drop correlations for horizontal and vertical two-phase pipe flow, in: European Two-Phase Group Meeting, Ispra, Italy, 1979.

[11] H. Müller-Steinhagen, K. Heck, A simple friction pressure drop correlation for two-phase flow in pipes, Chem. Eng. Process. Process Intensif. 20 (1986) 297–308, https://doi.org/10.1016/0255-2701(86)80008-3.

[12] C. Keepaiboon, P. Thiangtham, O. Mahian, A.S. Dalkiliç, S. Wongwises, Pressure drop characteristics of R134a during flow boiling in a single rectangular micro-channel, Int. Commun. Heat Mass Transf. 71 (2016) 245–253, https://doi.org/10.1016/j.icheatmasstransfer.2015.12.013.

[13] P. Rollmann, K. Spindler, New models for heat transfer and pressure drop during flow boiling of R407C and R410A in a horizontal microfin tube, Int. J. Therm. Sci. 103 (2016) 57–66, https://doi.org/10.1016/j.ijthermalsci.2015.11.010.

[14] L. Ming Pan, R. Gang Yan, H. Jie Huang, H. He, P. Fei Li, Experimental study on the flow boiling pressure drop characteristics in parallel multiple microchannels, Int. J. Heat Mass Transfer 116 (2018) 642–654, https://doi.org/10.1016/j.ijheatmasstransfer.2017.09.033.

[15] W. Zeng, Z. Du, X. Liu, Z. Tian, New generalized flow boiling heat transfer and frictional pressure drop correlations for R32, Int. J. Refrig. (2021) 634–644, https://doi.org/10.1016/j.ijrefrig.2021.02.025.
[16] F. Nie, S. Yan, H. Wang, C. Zhao, Y. Zhao, M. Gong, A universal correlation for predicting two-phase frictional pressure drop in horizontal tubes based on machine learning, Int. J. Multiphase Flow 160 (2023) 104377, https://doi.org/10.1016/j.ijmultiphaseflow.2022.104377.
[17] M.A. Moradkhani, S.H. Hosseini, M. Song, Comprehensive modeling of frictional pressure drop during carbon dioxide two-phase flow inside channels using intelligent and conventional methods, Chin. J. Chem. Eng. 63 (2023) 108–119, https://doi.org/10.1016/j.cjche.2023.05.001.
[18] S.-M. Kim, J. Kim, I. Mudawar, Flow condensation in parallel micro-channels–part 1: experimental results and assessment of pressure drop correlations, Int. J. Heat Mass Transf. 55 (2012) 971–983, https://doi.org/10.1016/j.ijheatmasstransfer.2011.10.013.
[19] J. Lee, I. Mudawar, Two-phase flow in high-heat-flux micro-channel heat sink for refrigeration cooling applications: part I - pressure drop characteristics, Int. J. Heat Mass Transf. 48 (2005) 928–940, https://doi.org/10.1016/j.ijheatmasstransfer.2004.09.018.
[20] J. Lee, I. Mudawar, Two-phase flow in high-heat-flux micro-channel heat sink for refrigeration cooling applications: part II - heat transfer characteristics, Int. J. Heat Mass Transf. 48 (2005) 941–955, https://doi.org/10.1016/j.ijheatmasstransfer.2004.09.019.
[21] S. Mehdi, M. Borumand, G. Hwang, Accurate and robust predictions of pool boiling heat transfer with micro-structured surfaces using probabilistic machine learning models, Int. J. Heat Mass Transf. 226 (2024) 125487.
[22] I. Mudawar, S.J. Darges, V.S. Devahdhanush, Prediction technique for flow boiling heat transfer and critical heat flux in both microgravity and earth gravity via artificial neural networks (ANNs), Int. J. Heat Mass Transf. 220 (2024), https://doi.org/10.1016/j.ijheatmasstransfer.2023.124998.
[23] Ş. Sezer, C. Sezer, A. Celen, A. Bacak, A.S. Dalkılıç, Investigation on the heat transfer and pressure loss of flow boiling in smooth and microfin tubes using machine learning methods, J. Therm. Anal. Calorim. 149 (2024) 15121–15141, https://doi.org/10.1007/s10973-024-13794-1.
[24] Y. Qiu, D. Garg, S.M. Kim, I. Mudawar, C.R. Kharangate, Machine learning algorithms to predict flow boiling pressure drop in mini/micro-channels based on universal consolidated data, Int. J. Heat Mass Transf. 178 (2021), https://doi.org/10.1016/j.ijheatmasstransfer.2021.121607.
[25] I. Mudawar, S.J. Darges, V.S. Devahdhanush, M.M. Hasan, H.K. Nahra, R. Balasubramaniam, J.R. Mackey, Pressure drop characteristics and prediction techniques (models/correlations and artificial neural networks) for microgravity flow boiling onboard the international Space Station, Int. J. Heat Mass Transf. 240 (2025), https://doi.org/10.1016/j.ijheatmasstransfer.2024.126593.
[26] R.M. Neal, Bayesian learning for neural networks 118, Springer Science & Business Media, 1995.
[27] M. Welling, D. Bren, Y.W. Teh, Bayesian learning via stochastic gradient langevin dynamics, in: Proceedings of the 28th International Conference on Machine Learning (ICML-11), 2011, pp. 681–688.
[28] A.B. Çolak, A. Bacak, Y. Karakoyun, A. Koca, A.S. Dalkilic, Machine learning application with Bayesian regularization for predicting pressure drop in R134a's annular evaporation and condensation, J. Braz. Soc. Mech. Sci. Eng. 47 (2025), https://doi.org/10.1007/s40430-025-05527-8.
[29] J. Li, C.R. Kharangate, Physics-assisted machine learning models for predicting Pool boiling critical heat flux for cryogenic fluids, ASME J. Heat and Mass Transf. 147 (2025), https://doi.org/10.1115/1.4067339.
[30] A. Mondal, S.L. Sharma, Physics-informed machine learning-aided framework for entrainment fraction in gas-liquid two-phase annular flow, Appl. Therm. Eng. 296 (2026) 130778, https://doi.org/10.1016/j.applthermaleng.2026.130778.
[31] F.B. Golezani, J. Li, F. Naderi, A. Meylikhov, L.M. Pirnstill, S.M. Kim, I. Mudawar, C. Kharangate, Enhanced prediction of condensation pressure drop in mini and microchannels using physics-assisted machine learning, Int. J. Heat Mass Transf. 255 (2026), https://doi.org/10.1016/j.ijheatmasstransfer.2025.127838.
[32] S.M. Kim, I. Mudawar, Review of databases and predictive methods for pressure drop in adiabatic, condensing and boiling mini/micro-channel flows, Int. J. Heat Mass Transf. 77 (2014) 74–97, https://doi.org/10.1016/j.ijheatmasstransfer.2014.04.035.
[33] S.-M. Kim, J. Kim, I. Mudawar, Flow condensation in parallel micro-channels – part 1: experimental results and assessment of pressure drop correlations, Int. J. Heat Mass Transf. 55 (2012) 971–983, https://doi.org/10.1016/j.ijheatmasstransfer.2011.10.013.
[34] W.H. McAdams, W.K. Woods, L.C. Heroman Jr., Vaporization inside horizontal tubes—II benzene-oil mixtures, Trans. ASME 64 (1942) 193–200, https://doi.org/10.1115/1.4019013.
[35] B.W. F Davidson, P.H. Hardie, C.G. R Humphreys, A.A. Markson, A.R. Mumford, T. Ravese, Studies of heat transmission through boiler tubing at pressures from 500 to 3300 pounds, J. Fluids Eng. 65 (1943) 553–579, https://doi.org/10.1115/1.4018835.
[36] W.W. Akers, H.A. Deans, O.K. Crosser, Condensing heat transfer within horizontal tubes, Chem. Eng. Prog. 54 (1958) 89–90.
[37] A. Cicchitti, C. Lombardi, M. Silvestri, G. Soldaini, R. Zavattarelli, Two-Phase Cooling Experiments: Pressure Drop, Heat Transfer and Burnout Measurements, Centro Informazioni Studi Esperienze, Milan, 1959.
[38] W.L. Owens, Two-phase pressure gradient, in: Int. Dev. Heat Transfer, Pt. II, ASME, New York, NY, USA, 1961.
[39] A.E. Dukler, M. Wicks III, R.G. Cleveland, Frictional pressure drop in two-phase flow: B. An approach through similarity analysis, AIChE J 10 (1964) 44–51, https://doi.org/10.1002/aic.690100117.
[40] D.R.H. Beattie, P.B. Whalley, A simple two-phase frictional pressure drop calculation method, Int. J. Multiphase Flow 8 (1982) 83–87, https://doi.org/10.1016/0301-9322(82)90009-X.
[41] S. Lin, C.C.K. Kwok, R.-Y. Li, Z.-H. Chen, Z.-Y. Chen, Local frictional pressure drop during vaporization of R-12 through capillary tubes, Int. J. Multiphase Flow 17 (1991) 95–102, https://doi.org/10.1016/0301-9322(91)90072-B.
[42] M.M. Awad, Y.S. Muzychka, Effective property models for homogeneous two-phase flows, Exp. Therm. Fluid Sci. 33 (2008) 106–113, https://doi.org/10.1016/j.expthermflusci.2008.07.006.
[43] S.M. Zivi, Estimation of steady-state steam void-fraction by means of the principle of minimum entropy production, J. Heat Transfer 86 (1964) 247–251, https://doi.org/10.1115/1.3687113.
[44] C.R. Kharangate, I. Mudawar, M.M. Hasan, Experimental and theoretical study of critical heat flux in vertical upflow with inlet vapor void, Int. J. Heat Mass Transf. 55 (2012) 360–374, https://doi.org/10.1016/j.ijheatmasstransfer.2011.09.028.
[45] K. Mishima, T. Hibiki, Some characteristics of air-water two-phase flow in small diameter vertical tubes, Int. J. Multiphase Flow 22 (1996) 703–712, https://doi.org/10.1016/0301-9322(96)00010-9.
[46] H.J. Lee, S.Y. Lee, Pressure drop correlations for two-phase flow within horizontal rectangular channels with small heights, Int. J. Multiphase Flow 27 (2001) 783–796, https://doi.org/10.1016/S0301-9322(00)00050-1.
[47] C.Y. Yang, R.L. Webb, Friction pressure drop of R-12 in small hydraulic diameter extruded aluminum tubes with and without micro-fins, Int. J. Heat Mass Transf. 39 (1996) 801–809, https://doi.org/10.1016/0017-9310(95)00151-4.
[48] C.C. Wang, C.S. Chiang, D.C. Lu, Visual observation of two-phase flow pattern of R-22, R-134a, and R-407C in a 6.5-mm smooth tube, Exp. Therm. Fluid Sci. 15 (1997) 395–405, https://doi.org/10.1016/S0894-1777(97)00007-1.
[49] W. Li, Z. Wu, A general correlation for adiabatic two-phase pressure drop in micro/mini-channels, Int. J. Heat Mass Transf. 53 (2010) 2732–2739, https://doi.org/10.1016/j.ijheatmasstransfer.2010.02.029.
[50] W. Li, Z. Wu, Generalized adiabatic pressure drop correlations in evaporative micro/mini-channels, Exp. Therm. Fluid Sci. 35 (2011) 866–872, https://doi.org/10.1016/j.expthermflusci.2010.07.005.
[51] W. Qu, I. Mudawar, Measurement and prediction of pressure drop in two-phase micro-channel heat sinks, Int. J. Heat Mass Transf. 46 (2003) 2737–2753, https://doi.org/10.1016/S0017-9310(03)00044-9.
[52] D.S. Jung, R. Radermacher, Prediction of pressure drop during horizontal annular flow boiling of pure and mixed refrigerants, Int. J. Heat Mass Transf. 32 (1989) 2435–2446, https://doi.org/10.1016/0017-9310(89)90203-2.
[53] Y.Y. Yan, T.F. Lin, Evaporation heat transfer and pressure drop of refrigerant R-134a in a small pipe, Int. J. Heat Mass Transf. 41 (1998) 4183–4194, https://doi.org/10.1016/S0017-9310(98)00127-6.
[54] T.N. Tran, M.-C. Chyu, M.W. Wambsganss, D.M. France, Two-phase pressure drop of refrigerants during flow boiling in small channels: an experimental investigation and correlation development, Int. J. Multiphase Flow 26 (2000) 1739–1754, https://doi.org/10.1016/S0301-9322(99)00119-6.
[55] W. Yu, D.M. France, M.W. Wambsganss, J.R. Hull, Two-phase pressure drop, boiling heat transfer, and critical heat flux to water in a small-diameter horizontal tube, Int. J. Multiphase Flow 28 (2002) 927–941, https://doi.org/10.1016/S0301-9322(02)00019-8.
[56] L. Sun, K. Mishima, Evaluation analysis of prediction methods for two-phase flow pressure drop in mini-channels, Int. J. Multiphase Flow 35 (2009) 47–54, https://doi.org/10.1016/j.ijmultiphaseflow.2008.08.003.
[57] X. Ma, C. Hu, X. Ji, X. Yang, N. Xu, Y. Zhang, J. Wei, Y. Feng, B. Sundén, Flow boiling frictional pressure drop inside micro/mini-channels: a new general model and experimental investigation, Appl. Therm. Eng. 247 (2024), https://doi.org/10.1016/j.applthermaleng.2024.123111.
[58] J. Moreno Quibén, J.R. Thome, Flow pattern based two-phase frictional pressure drop model for horizontal tubes, part II: new phenomenological model, Int. J. Heat Fluid Flow 28 (2007) 1060–1072, https://doi.org/10.1016/j.ijheatfluidflow.2007.01.004.
[59] L. Wojtan, T. Ursenbacher, J.R. Thome, Investigation of flow boiling in horizontal tubes: part I - a new diabatic two-phase flow pattern map, Int. J. Heat Mass Transf. 48 (2005) 2955–2969, https://doi.org/10.1016/j.ijheatmasstransfer.2004.12.012.
[60] L. Cheng, G. Ribatski, J. Moreno Quibén, J.R. Thome, New prediction methods for CO_2 evaporation inside tubes: part I - a two-phase flow pattern map and a flow pattern based phenomenological model for two-phase flow frictional pressure drops, Int. J. Heat Mass Transf. 51 (2008) 111–124, https://doi.org/10.1016/j.ijheatmasstransfer.2007.04.002.
[61] D. Shiferaw, M. Mahmoud, T.G. Karayiannis, D.B.R. Kenning, One-dimensional semimechanistic model for flow boiling pressure drop in small to micro passages, Heat Transfer Eng. 32 (2011) 1150–1159, https://doi.org/10.1080/01457632.2011.562726.
[62] S. Lee, I. Mudawar, Enhanced model for annular flow in micro-channel heat sinks, including effects of droplet entrainment/deposition and core turbulence, Int. J. Heat Mass Transf. 133 (2019) 510–530, https://doi.org/10.1016/j.ijheatmasstransfer.2018.12.074.
[63] A.W. Mauro, L. Viscito, R. Revellin, Void fraction and pressure gradient model for an adiabatic symmetric annular developed flow with entrainment, Int. J. Multiphase Flow 153 (2022), https://doi.org/10.1016/j.ijmultiphaseflow.2022.104126.
[64] G.B. Wallis, One-Dimensional Two-Phase Flow, McGraw-Hill, New York, 1969.

[65] H. Blasius, Das Aehnlichkeitsgesetz bei Reibungsvorgangen Flftssigkeiten, Mitteilungen Über Forschungsarbeiten Auf Dem Gebiete Des Ingenieurwesens (1913) 1–41.

[66] A.W. Mauro, A.F. Passarelli, F. Pelella, L. Viscito, A mechanistic predictive model for pressure drop and void fraction calculation in two-phase flows and annular flow regime, Exp. Thermal Fluid Sci. 170 (2026), https://doi.org/10.1016/j.expthermflusci.2025.111590.

[67] Y. Zhu, X. Wu, R. Zhao, R32 flow boiling in horizontal mini channels: part II flow-pattern based prediction methods for heat transfer and pressure drop, Int. J. Heat Mass Transf. 115 (2017) 1233–1244, https://doi.org/10.1016/j.ijheatmasstransfer.2017.07.099.

[68] A.M. Lezzi, A. Niro, G.P. Beretta, Experimental data on CHF for forced convection water boiling in long horizontal capillary tubes, in: International Heat Transfer Conference Digital Library, Begel House Inc., 1994.

[69] T.Nhon. Tran, Pressure Drop and Heat Transfer Study of Two-Phase Flow in Small Channels, Texas Tech University, 1998.

[70] X. Huo, Experimental Study of Flow Boiling Heat Transfer in Small Diameter Tubes, London South Bank University, 2005.

[71] W. Owhaib, C. Martín-Callizo, B. Palm, Two-phase flow pressure drop of R-134A in a vertical circular mini/micro channel, in: ASME Sixth Int. Conf. On Nanochannels, Microchannels, and Minichannels, Germany, 2008, pp. 343–353.

[72] H. Hu, G. Ding, X. Huang, B. Deng, Y. Gao, Pressure drop during horizontal flow boiling of R410A/oil mixture in 5 mm and 3 mm smooth tubes, Appl. Therm. Eng. 29 (2009) 3353–3365, https://doi.org/10.1016/j.applthermaleng.2009.05.011.

[73] M. Ducoulombier, Ebullition convective du dioxyde de carbone - étude expérimentale en micro-canal, Institut National des Sciences Appliquées (INSA) de Lyon, France, 2010.

[74] C.B. Tibiriçá, G. Ribatski, Two-phase frictional pressure drop and flow boiling heat transfer for R245fa in a 2.32-mm tube, Heat Transfer Eng. 32 (2011) 1139–1149, https://doi.org/10.1080/01457632.2011.562725.

[75] C.B. Tibiriçá, J. Diniz da Silva, G. Ribatski, Experimental investigation of flow boiling pressure drop of R134a in a microscale horizontal smooth tube, J. Therm. Sci. Eng. Appl. 3 (2011) 011006, https://doi.org/10.1115/1.4003728.

[76] J. Wu, T. Koettig, C. Franke, D. Helmer, T. Eisel, F. Haug, J. Bremer, Investigation of heat transfer and pressure drop of CO2 two-phase flow in a horizontal minichannel, Int. J. Heat Mass Transf. 54 (2011) 2154–2162, https://doi.org/10.1016/j.ijheatmasstransfer.2010.12.009.

[77] M.H. Maqbool, B. Palm, R. Khodabandeh, Flow boiling of ammonia in vertical small diameter tubes: two phase frictional pressure drop results and assessment of prediction methods, Int. J. Therm. Sci. 54 (2012) 1–12, https://doi.org/10.1016/j.ijthermalsci.2011.11.018.

[78] J. Qiu, H. Zhang, X. Yu, Y. Qi, J. Lou, X. Wang, Experimental investigation of flow boiling heat transfer and pressure drops characteristic of R1234ze(E), R600a, and a mixture of R1234ze(E)/R32 in a horizontal smooth tube, Adv. Mech. Eng. 7 (2015) 1–12, https://doi.org/10.1177/1687814015606311.

[79] G.A. Longo, S. Mancin, G. Righetti, C. Zilio, Saturated flow boiling of HFC134a and its low GWP substitute HFO1234ze(E) inside a 4 mm horizontal smooth tube, Int. J. Refrig. 64 (2016) 32–39, https://doi.org/10.1016/j.ijrefrig.2016.01.015.

[80] J. Garcia Pabon, A. Khosravi, R. Nunes, L. Machado, Experimental investigation of pressure drop during two-phase flow of R1234yf in smooth horizontal tubes with internal diameters of 3.2 mm to 8.0 mm, Int. J. Refrig. 104 (2019) 426–436, https://doi.org/10.1016/j.ijrefrig.2019.05.019.

[81] Z. Liang, J. Linlin, Liu Jianhua, Y. Yunxiao, Z. Jiawen, Research on pressure drop characteristics of CO 2 flow boiling based on flow pattern in horizontal Minichannel, Heat and Mass Transf. 56 (2020) 2939–2952, https://doi.org/10.1007/s00231-020-02904-y.

[82] Y. Xu, Z. Yan, L. Li, Experimental investigation on flow boiling heat transfer and pressure drop of a low-gwp refrigerant r1234ze(E) in a horizontal minichannel, Energies (Basel) 14 (2021), https://doi.org/10.3390/en14185972.

[83] Y. Xu, Z. Yan, L. Li, Flow boiling heat transfer, pressure drop and flow patterns of the environmentally friendly refrigerant R1234yf for cooling avionics, Appl. Therm. Eng. 209 (2022), https://doi.org/10.1016/j.applthermaleng.2022.118301.

[84] M.A.H. Mudhafar, H.Y. Pan, The fluid flow and heat transfer characteristics of R-32 in a small tube, Int. J. Refrig. 139 (2022) 204–213, https://doi.org/10.1016/j.ijrefrig.2022.03.033.

[85] J. Diehl de Oliveira, J.B. Copetti, E.M. Cardoso, R. Rodrigues de Souza, Flow boiling pressure drop of R-1270 in 1.0 mm tube, Appl. Therm. Eng. 231 (2023), https://doi.org/10.1016/j.applthermaleng.2023.120885.

[86] G.A. Longo, S. Mancin, G. Righetti, C. Zilio, Flow boiling heat transfer capabilities of R134a low GWP substitutes inside a 4 mm id horizontal smooth tube: R600a and R152a, Heat Mass Transf. 60 (2024) 1787–1805, https://doi.org/10.1007/s00231-020-02991-x.

[87] J.M. Quibén, L. Cheng, R.J. da Silva Lima, J.R. Thome, Flow boiling in horizontal flattened tubes: Part I–Two-phase frictional pressure drop results and model, Int. J. Heat Mass Transf. 52 (2009) 3634–3644.

[88] N.H. Kim, E.J. Lee, H.W. Byun, Evaporation heat transfer and pressure drop of R-410A in flattened smooth tubes having different aspect ratios, Int. J. Refrig. (2013) 363–374, https://doi.org/10.1016/j.ijrefrig.2012.10.001.

[89] J. Li, D. Su, M. Li, Q. Wang, C. Dang, J. Peng, Experimental study of flow boiling characteristics of R454B in an open microchannel with micro-nano composite structured surfaces, Appl. Therm. Eng. 280 (2025), https://doi.org/10.1016/j.applthermaleng.2025.128499.

[90] H. Cheol, H.K. Moo, Pressure drop, boiling heat transfer and flow patterns during flow boiling in a single microchannel, Heat Transf. Eng. 28 (2007) 730–737, https://doi.org/10.1080/01457630701328213.

[91] S. Azarhazin, B. Sajadi, H. Fazelnia, M.A. Akhavan Behabadi, S. Zakeralhoseini, Boiling heat transfer coefficient and pressure drop of R1234yf flow inside smooth flattened tubes: an experimental study, Appl. Therm. Eng. 165 (2020), https://doi.org/10.1016/j.applthermaleng.2019.114595.

[92] U. Soupremanien, S. Le Person, M. Favre-Marinet, Y. Bultel, Influence of the aspect ratio on boiling flows in rectangular mini-channels, Exp. Therm. Fluid Sci. 35 (2011) 797–809, https://doi.org/10.1016/j.expthermflusci.2010.06.014.

[93] S.J. Qin, B. De Chen, X. Yan, Z.J. Xiao, Y.P. Huang, Experimental investigation on frictional pressure drop of water in vertical rectangular channel, Nucl. Eng. Des. 250 (2012) 567–572, https://doi.org/10.1016/j.nucengdes.2012.05.035.

[94] A. Candan, B. Markal, O. Aydin, M. Avci, Saturated flow boiling characteristics in single rectangular minichannels: effect of aspect ratio, Exp. Heat Transf. 31 (2018) 531–551, https://doi.org/10.1080/08916152.2018.1463305.

[95] B. Markal, A. Candan, O. Aydin, M. Avci, Experimental investigation of flow boiling in single minichannels with low mass velocities, Int. Commun. Heat Mass Transf. 98 (2018) 22–30, https://doi.org/10.1016/j.icheatmasstransfer.2018.08.002.

[96] J. Lee, I. Mudawar, Two-phase flow in high-heat-flux micro-channel heat sink for refrigeration cooling applications: part II—heat transfer characteristics, Int. J. Heat Mass Transf. 48 (2005) 941–955.

[97] W. Qu, I. Mudawar, Transport phenomena in two-phase micro-channel heat sinks, J. Electron. Packag. 126 (2004) 213–224, https://doi.org/10.1115/1.1756145.